

Department of Physics and Astronomy

University of Heidelberg

Master thesis

in Physics

submitted by

Marcus Theisen

born in Würselen

2017

Adiabatic Driving Protocols
for
Few-Level Quantum Systems

This Master thesis has been carried out by Marcus Theisen

at the

Institute for Theoretical Physics

under the supervision of

Priv.-Doz. Sandro Wimberger

Adiabatische Kontroll-Protokolle für Quantensysteme mit wenigen Zuständen:

Diese Arbeit beschäftigt sich mit sogenannten „shortcuts to adiabaticity“ Protokollen, deren weitere Entwicklung eine effiziente Kontrolle von Quantensystemen verspricht. Das Ziel dieser Klasse von Protokollen ist es, die instantanen Eigenzustände eines Quantensystemen exakt zu treiben, sodass keine Übergänge zwischen ihnen stattfinden.

Der Fokus bisherige Betrachtungen lag auf exakten Lösungen für Zwei- und Drei-Niveau-Systemen. In dieser Arbeit analysieren wir das exakte „super-adiabatische“ Protokoll für ein Drei-Zustands-Modell und diskutieren dessen Aufspaltung in lokale Zwei-Zustands-Korrekturen. Dafür zeigen wir zuerst, dass das exakte Kontrollprotokoll den Zustandsübergängen durch Impulse, die an deren Kreuzungen im zeitabhängigen Spektrum liegen, entgegenwirkt. Die asymptotische Form dieser Impulse wird durch Potenzgesetze beschrieben und verbietet somit eine natürliche Definition von Separabilität. Dennoch diskutieren wir die Möglichkeit der sequenzierten Kontrolle durch idealisierte Landau-Zener-Korrekturen. Wir finden, dass der Fehler des „sequenziellen“ Protokolls als Potenz des Abstand zwischen den individuellen Kreuzungen skaliert. Damit ist die Genauigkeit des präsentierten Protokolls abhängig vom System. Schlussendlich schlagen wir verschiedene experimentelle Realisierungsmöglichkeiten vor und zeigen, dass diese Art sequentieller Kontrolle theoretisch auf Systeme mit beliebig vielen Zuständen erweiterbar ist.

Adiabatic Driving Protocols for Few-Level Quantum Systems:

In this thesis we consider a set of protocols collectively known as “shortcuts to adiabaticity” which suggest that efficient, that is rapid and robust, quantum control is possible. This class of control protocols allows to steer the instantaneous eigenstates of a quantum system exactly, without inducing transitions between them.

The ultimate goal of this thesis is to study the decomposition of these “super-adiabatic” protocols for few-level systems into local two-level correction terms. Therefore we explicitly construct a three-state model whose energy spectrum exhibits multiple avoided crossings. We then show that the time profiles of the exact control Hamiltonian are characterized by peaks centered around the crossing times. These peaks are found to scale as power laws in the asymptotic time limit which in principle invalidates the hypothesis of perfect separability. Nonetheless, we address the problem from a pragmatic point of view and study the possibility of constructing a “sequential control” protocol from local Landau-Zener corrections acting at the avoided crossings. We find that the error made by the proposed protocol scales as a power of the inter-crossing separation. Finally, we present various experimental test scenarios and show that the generalization of the protocol to few-level systems is in principle possible.

Contents

1	Introduction	9
2	Theory	13
2.1	Foundations of Quantum Mechanics	14
2.2	Two-State System	15
2.2.1	Landau-Zener Problem	17
2.3	Control Theory: Transitionless Quantum Driving	19
2.3.1	General Spin System	21
3	Modelling a Three-State System	25
3.1	Time-Symmetric Version	26
3.2	Counterdiabatic Control Hamiltonian	27
3.2.1	Analytically Solvable Limits	28
3.2.2	Numerical Shape of Control Pulses	29
3.2.3	Weak Coupling Limit	31
3.2.4	Asymptotic Behaviour	31
3.3	Time-Asymmetric Version	32
3.3.1	Sequential Control Hamiltonian	34
4	Ground State Dynamics	37
4.1	Numerical Details	38
4.2	Super-Adiabatic Protocol	39
4.2.1	Robustness	40
4.3	Sequential Control Protocol	41
4.3.1	Probability of Non-Adiabaticity	44
5	Perspectives	47
5.1	Experimental Realization	48
5.2	Four-Level System	49
6	Conclusion	53
	Appendix	57
A	Derivation of Landau-Zener Formula	59
B	Derivation of CD Hamiltonian at $t = 0$	61

C Time-Independent Perturbation Theory	63
D Bibliography	67

Acronyms

AC Avoided Crossing

CD Counter-Diabatic

LZ Landau-Zener

QBism Quantum Bayesianism

QuBit Quantum Bit

RAP Rapid Adiabatic Passage

SA Super-Adiabatic

SC Sequential Control

STIRAP STImulated Raman Adiabatic Passage

TIPT Time-Independent Perturbation Theory

TQD Transitionless Quantum Driving

1 Introduction

Humanity has always longed for control over nature. By nature I mean ourselves, the human’s body and mind, as well as its surrounding environment from the smallest to the largest scales. Now is the time when mankind has both sufficient knowledge and the experimental experties to manipulate these systems at a quantum level. In particular, the ability to control the dynamics of quantum systems has pushed forward the development of quantum technologies like quantum simulators and universal quantum computers. Since this thesis deals with the realization of the control schemes just mentioned, with the results already being published (Theisen et al., 2017), I like to stress that it is also time to think about its proper use. As it is my personal stance, I want to advocate utilizations that are as ethical and humanitarian as possible thereby ensuring the novel (computational) power to be well distributed.

At the basis for sophisticated control schemes lies the understanding of fundamental processes that govern the system to be controlled. Although quantum theory provides us with the mathematical toolkit to describe these processes the variety of interpretations of quantum mechanics has been constantly growing since its development. Only recently, renewed interest in *foundations of quantum mechanics* aims to provide a modern axiomatisation of quantum theory in terms of information. Two promising approaches are Quantum Thermodynamics, which characterises quantum theory by its information content using the notion of entropy (Goold et al., 2016), and Quantum Bayesianism, which refuses an objective realism by including an observer in the theory (Caves et al., 2002). In QBism, the observer takes the role of an agent who assigns and measures states according to its subjective knowledge. Both ideas are conceptionally useful in the sense that they focus on the computational aspects of quantum theory and make statements about the amount of information that can be stored and accessed in a quantum system.

Given a sound quantum formalism, the task is to develop reliable and experimentally realizable protocols that produce a fixed behaviour (Dong and Petersen, 2010). In the field of quantum computation much effort has been invested into the efficient implementation of quantum gates. They form the analogon to logical gates known from classical computation and usually are designed for Qubits, the most basic entity of information in quantum theory.

In the more general framework of quantum control theory, time-dependent control protocols, that go by the collective name of shortcuts to adiabaticity (Torrontegui et al., 2013), have been attracting attention. Synonyms are transitionless quantum driving theory (TQD) (Berry, 2009), superadiabatic (SA) (Bason et al., 2012) and counterdiabatic (CD) control protocols (Demirplak and Rice, 2003). The core idea is that, given an initial Hamiltonian $H(t)$, it is always possible to find a correcting term $H_{CD}(t)$ which cancels non-adiabatic effects. The combined Hamiltonian $H(t) + H_{CD}(t)$ then drives the instantaneous eigenstates of $H(t)$ exactly, i.e., adiabatically.

The TQD algorithm suffers of two main weaknesses. First of all, while in principle it provides the CD control fields for quantum systems of arbitrarily many energy levels, going beyond the two-level case often becomes analytically infeasible, and must be treated numerically. To this extent, time-optimal control theory (Glaser et al.,

2015) has been applied to find the optimal shape of the control pulses. Secondly, even when the CD corrections are found, they might require physical interactions which are not present in the original Hamiltonian, leading to difficulties in the experimental realizations. Both issues will be of concern here.

Still, exact analytical results have been produced and tested for some specific problems. The solvable Landau-Zener-Majorana-Stückelberg (LZ for brevity) model (Landau, 1932; Zener, 1932; Majorana, 1932; Stückelberg, 1932) plays a central role in probing TQD protocols on idealized two-level scenarios (Bason et al., 2012; Malossi et al., 2013). A major achievement in three-level dynamics is the insight that SA control protocols improve the efficiency of stimulated Raman adiabatic passage (STIRAP) schemes in terms of fidelity, robustness and transfer time (Baksic et al., 2016; Zhou et al., 2017). In addition, exact CD fields have been found for scale-invariant dynamical processes (del Campo, 2013; Deffner et al., 2014).

In this thesis we will study the application of the SA protocol to a three-level system in which the ground state undergoes a sequence of avoided crossings (ACs) in the time-dependent energy spectrum. The motivation behind this choice resides in the fact that the transition probability between two states is extreme enhanced in the vicinity of an AC. As adiabatic control theory ultimately deals with the suppression of these non-adiabatic transitions, the natural question we pose is whether the full control problem can be decomposed into the sum of local SA protocols acting at the individual ACs. Thus, the approach which we shall adopt here differs from the typical quest for shortcuts to adiabaticity. Rather than demanding exact adiabatic evolution, our main concern is to study the possibility of constructing a sequential control (SC) Hamiltonian from single AC corrections, and to test the validity of such an approximation. Ideally, the ACs can be treated as LZ-type interactions which usually yields a good local approximation to more complex spectra (Shevchenko et al., 2010).

The structure of this thesis is as follows. After a brief review of the TQD theory and its application to the control of a single LZ event in Chapter 2, we model a three-level system suited for studies on SC in Chapter 3. We analytically calculate the control fields for limiting cases, compute the exact controls numerically and finally discuss their long-range properties using perturbative arguments. Possible construction schemes for the SC protocols are presented with focus on experimental realizability. The effects of the exact CD and approximate SC protocols on the ground state dynamics are presented in Chapter 4. Here, by numerical integration of the time-dependent Schrödinger equation the dependency of the protocol's error on the time separation between the crossings is inferred. Then in Chapter 5, we first discuss aspects concerning possible experimental implementations of the three-level system and conclude by generalizing the ideal of sequential control to a four-level system. Numerical results are given. In the closing Chapter 6, the results are summarized and future prospects are discussed.

2 Theory

In this chapter, I present the theoretical background necessary for the understanding of this thesis. First, I recapitulate the tenets and most basic features of quantum mechanics introducing important concepts and notions. These are then used to discuss the two-state quantum system, its mathematical properties and physical time evolution. Finally, I give a short description of transitionless quantum driving theory and discuss its application to general spin systems, particularly to the Landau-Zener model.

2.1 Foundations of Quantum Mechanics

Let us begin by defining *quantum states*. The state space of an n -level quantum systems is spanned by the finite-dimensional (complex) Hilbert space $\mathcal{H}(\mathbb{C}, n)$. The elements of that space are Hilbert space vectors which we denote in Dirac bra-ket notation as $|\Psi\rangle$.

Let us next think about the information about this state that is accessible by experimental measurement techniques. What is inferred by repeated measurements are *transition probabilities* $P_{i \rightarrow j}$ between two quantum states $|\Psi_i\rangle$ and $|\Psi_j\rangle$. In the probabilistic interpretation of quantum mechanics it is defined by the inner product of the respective states

$$P_{i \rightarrow j} = \frac{|\langle \Psi_i | \Psi_j \rangle|^2}{\langle \Psi_i | \Psi_i \rangle \langle \Psi_j | \Psi_j \rangle}. \quad (2.1)$$

Clearly, this quantity does not depend on the complex phase of a particular Hilbert space vector $|\Psi\rangle$; we say its phase is *unobservable*. Conventionally, choosing normalized states by demanding $\langle \Psi | \Psi \rangle = 1$ it is taming to assume that quantum states correspond to *rays* in Hilbert space. A ray is defined as the equivalence class $[\Psi]$ of states:

$$(|\Psi\rangle \sim |\Psi'\rangle) \Leftrightarrow (|\Psi\rangle = e^{i\alpha} |\Psi'\rangle), \quad \alpha \in \mathbb{R}. \quad (2.2)$$

Here, α is the unobservable *global phase* of the state. In this sense $P_{i \rightarrow j}$ depends only on the equivalence classes $[\Psi_i]$ and $[\Psi_j]$. Formally spoken, the action of the unitary group $U(1)$ leaves the quantum state as we observe it invariant and constitutes a gauge symmetry of the first kind. As the measurement process involves the projection of states it is also called the *projective symmetry*. The quantum states therefore merely describe states of knowledge about the physical system at hand.

Note, that for any state belonging to the equivalence class $[\Psi]$, we can write its *decomposition* into a complete set of basis states $\{|\phi_i\rangle\}$ such that the *relative phases* between the expansion coefficients $c_i \in \mathbb{C}$ are well-defined and fixed

$$|\Psi\rangle = \sum_i^n c_i |\phi_i\rangle. \quad (2.3)$$

This allows the measurement of relative phases by interference experiments as interference is always of a ray with itself. On the contrary the notion of *superposition*

is ill-defined as there is simply no way to conveniently add two rays. Conventionally one introduces the normalization constraint that the total probability, i.e., the sum of all projection probabilities on the basis states $|\phi_i\rangle$, adds up to one:

$$\sum_i |c_i|^2 = 1. \quad (2.4)$$

Let us next regard how dynamic processes are described in quantum mechanics. For pure states time evolution is given by the Schrödinger equation

$$i\hbar\partial_t |\Psi(t)\rangle = H(t) |\Psi(t)\rangle, \quad (2.5)$$

where H is the Hamiltonian operator acting on Hilbert space *vectors*. Thus state propagation via the SE inevitably breaks the projective symmetry but contrarily gives rise to dynamic and geometric phases (Solem and Biedenharn, 1993).

The formal solution to the evolution equation (2.5) is nicely written in terms of the time evolution operator

$$U(t, t_0) = \mathcal{T} \exp\left\{-\frac{i}{\hbar} \int_{t_0}^t dt' H(t')\right\} \quad (2.6)$$

involving the time ordered matrix exponential, also known as the Dyson series, such that $|\Psi(t)\rangle = U(t, t_0) |\Psi(t_0)\rangle$ for $t > t_0$. As to describe a measurable quantity, i.e., an *observable*, H is usually chosen to be hermitian (Bender, 2007) and by the exponential map U is ensured to be unitary. The consequence of *unitarity* is that time evolution in quantum mechanics conserves the norm of a vector. Therefore unitary time evolution is *reversible* and *deterministic*, however, by virtue of Eq. (2.1) the measurement process makes quantum mechanics *probabilistic*.

2.2 Two-State System

The simplest non-trivial quantum system is constituted by two coupled energy levels. It constitutes the most basic entity of information in quantum theory, i.e., a *qubit*. Although it is well discussed in text books like Sakurai and Napolitano (2011) or Haken (1979) we will outline its basic features as it will play a central role in our studies of more complex systems. In particular the LZ model is presented as an idealized ACs event of two energy levels, which usually yields a good local approximation to more evolved spectra (Shevchenko et al., 2010).

For a given coordinatization (choice of coordinates) of the underlying Hilbert space $\mathcal{H}(\mathbb{C}, 2)$ any state $|\Psi\rangle$ can be represented by a linear combination of two complex basis vectors

$$|\Psi\rangle = c_1 |\phi_1\rangle + c_2 |\phi_2\rangle. \quad (2.7)$$

Linear operations can be represented by matrices acting on the state and in particular observables correspond to hermitian matrices. The *Pauli matrices*

$$\sigma_1 = \begin{pmatrix} 0 & 1 \\ 1 & 0 \end{pmatrix}, \quad \sigma_2 = \begin{pmatrix} 0 & -i \\ i & 0 \end{pmatrix}, \quad \sigma_3 = \begin{pmatrix} 1 & 0 \\ 0 & -1 \end{pmatrix}, \quad (2.8)$$

span that space of hermitian 2-by-2-matrices. They obey the commutation relation

$$[\sigma_i, \sigma_j] = 2i\varepsilon_{ijk}\sigma_k, \quad (2.9)$$

where ε_{ijk} is the Levi-Civita symbol. The conventional choice of basis for qubit states is the eigenbasis of σ_3 , whose eigenvectors

$$|\sigma_3; +\rangle \equiv |0\rangle = \begin{pmatrix} 1 \\ 0 \end{pmatrix}, \quad |\sigma_3; -\rangle \equiv |1\rangle = \begin{pmatrix} 0 \\ 1 \end{pmatrix} \quad (2.10)$$

have respective eigenvalues ± 1 . Here, the state labels 0 and 1 are reminiscent of the classical bit states. Defining the *Pauli vector* as $\boldsymbol{\sigma} = (\sigma_1, \sigma_2, \sigma_3)$, any observable A can be constructed as a linear combination of the Pauli matrices

$$A = a_0 I + \mathbf{a} \cdot \boldsymbol{\sigma} = \begin{pmatrix} a_0 + a_3 & a_1 - ia_2 \\ a_1 + ia_2 & a_0 - a_3 \end{pmatrix}, \quad (2.11)$$

where $a_i \in \mathbb{R}$. Further, I is the identity matrix and $\mathbf{a} = a\hat{\mathbf{n}}$ is a three-vector of length $a = |\mathbf{a}|$ and orientation $\hat{\mathbf{n}}$.

From the fundamental properties of the Pauli matrices (2.9), it follows directly that the two-state quantum system is closed under hermitian operations as stated mathematically by the *completeness relation*:

$$(\mathbf{a} \cdot \boldsymbol{\sigma})(\mathbf{a}' \cdot \boldsymbol{\sigma}) = (\mathbf{a} \cdot \mathbf{a}')I + i(\mathbf{a} \times \mathbf{a}') \cdot \boldsymbol{\sigma}. \quad (2.12)$$

From this we can compute the commutator of two observables

$$[A, A'] = 2i(\mathbf{a} \times \mathbf{a}') \cdot \boldsymbol{\sigma}. \quad (2.13)$$

Thus two observable A and A' commute if and only if \mathbf{a} and \mathbf{a}' are linear dependent, i.e., if $\hat{\mathbf{n}} = \hat{\mathbf{n}}'$.

Solving the eigenequation for A it turns out that the eigenvalues of A depend on the bias a_0 and the norm a , while computation of the eigenstates only involves the direction $\hat{\mathbf{n}}$. Interpreting $\hat{\mathbf{n}}$ as a vector on the unit sphere S^2 in can be parameterized in spherical coordinates

$$\hat{\mathbf{n}} = \begin{pmatrix} \sin \theta \cos \phi \\ \sin \theta \sin \phi \\ \cos \theta \end{pmatrix}. \quad (2.14)$$

That is the eigenstates only depend on the two angles $0 \leq \theta < \pi$ and $0 \leq \phi < 2\pi$ and can conveniently be visualized as positions on the unit sphere S^2 , which is also called the *Bloch sphere*. We say, that the observable A measures the system along axis $\hat{\mathbf{n}}$ with possible measurement outcomes given by its eigenvalues

$$a_0 \pm a = a_0 \pm \sqrt{a_1^2 + a_2^2 + a_3^2}. \quad (2.15)$$

By the dot product in Eq. (2.11), which provides the mapping from the vector basis $\{\hat{\boldsymbol{x}}_i\}_{i=1,2,3}$ to the Pauli matrix basis, the eigenstates in bra-ket notation are given by

$$|A; +\rangle = \begin{pmatrix} \cos(\theta/2) \\ \sin(\theta/2)e^{i\phi} \end{pmatrix}, \quad |A; -\rangle = \begin{pmatrix} \sin(\theta/2)e^{-i\phi} \\ -\cos(\theta/2) \end{pmatrix}. \quad (2.16)$$

For $\theta = 0$ ($\theta = \pi$) the eigenstates of σ_3 are recovered. Therefore the qubit states $|0\rangle$ and $|1\rangle$ correspond to measurements of along the z -axis of the Bloch sphere. This further validates the synonymous notion of *spin basis* as they correspond to top and bottom points on the Bloch sphere.

Now, with the Bloch sphere as an easy-to-grasp visualization of a qubit's state space, continuous and norm-conserving transformation of states is intuitively given by rotations on the Bloch sphere. The corresponding unitary transformation on the state $|\Psi\rangle$ is given by the exponential map of a general hermitian matrix

$$\exp\{-iA\} = \exp\{-ia_0I\} \exp\{-i\boldsymbol{a} \cdot \boldsymbol{\sigma}\}. \quad (2.17)$$

As the state's global phase is unobservable we can discard the term involving a_0 . After identifying a with ϕ general rotations are written as

$$U_{\hat{\boldsymbol{n}}}(\phi) = \exp\{-i\phi\hat{\boldsymbol{n}} \cdot \boldsymbol{\sigma}\} = \cos(\phi)I - i\sin(\phi)\hat{\boldsymbol{n}} \cdot \boldsymbol{\sigma}. \quad (2.18)$$

This is Stone's theorem. It establishes a one-to-one correspondence between self-adjoint operators A acting on a Hilbert space \mathcal{H} and one-parameter families of unitary operators $U(\phi)$. Under the action of $U_{\hat{\boldsymbol{n}}}(\phi)$ a state is rotated around the axis $\hat{\boldsymbol{n}}$ by the angle ϕ .

After this review on the mathematical properties of the two-state system let us study the dynamics of physical systems described by the general Hamiltonian

$$H(t) = \frac{\hbar}{2} \begin{pmatrix} \omega(t) & \Delta(t) \\ \Delta^*(t) & -\omega(t) \end{pmatrix}. \quad (2.19)$$

Here, ω is a real-valued *energy sweep function* and Δ a complex *coupling*. As we explicitly extracted the Planck constant \hbar , both quantities are measured in units of inverse time $1/T$. Its eigenenergies are $E_{\pm} = \pm\hbar\sqrt{\omega^2 + |\Delta|^2}$ and instantaneous eigenstates $|E_{\pm}\rangle$ are given by Eq. (2.16). The usual parameterization of states is defined by

$$\tan\theta(t) = \frac{\Delta(t)}{\omega(t)} \quad \text{and} \quad \phi(t) = \arg\Delta(t). \quad (2.20)$$

2.2.1 Landau-Zener Problem

In the following let us solve the special case where the interaction is real and time-independent ($\dot{\Delta} = 0$) and the energy sweep function is linear $\omega(t) = \alpha t$ with $\alpha > 0$. Consequently, the paradigmatic Hamiltonian ($\hbar = 1$) reads

$$H_{LZ}(t) = \frac{1}{2} \begin{pmatrix} \alpha t & \Delta \\ \Delta & -\alpha t \end{pmatrix}. \quad (2.21)$$

This model is best understood by regarding its time-dependent energy spectrum as sketched in Fig. 2.1. On the basis of this idealized crossing event of two energy levels, let us introduce some nomenclature that will be useful in the general discussion of avoided crossings (ACs).

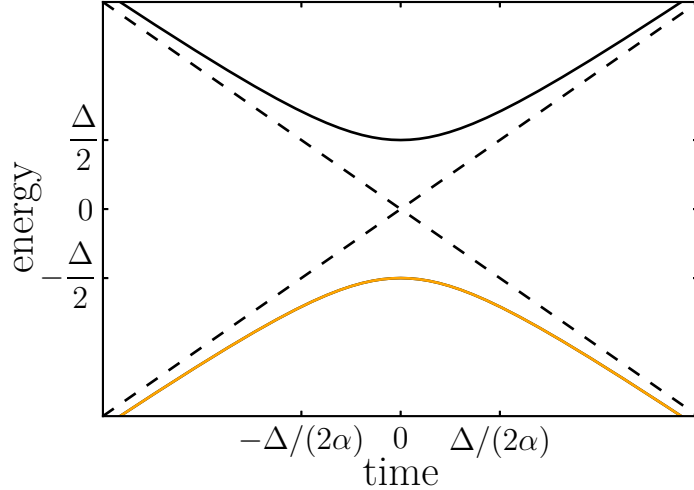


Figure 2.1: Schematic of the time-dependent spectrum of $H_{LZ}(t)$. Dashed and solid lines represent diabatic and adiabatic eigenstates, respectively. The temporal evolution of the ground state subject to superadiabatic control is given by the orange line.

Conventionally, we name the time-independent eigenstates of the uncoupled system ($\Delta = 0$) *diabates* and the instantaneous eigenstates of the coupled system *adiabates*. We denote them as $\{|n\rangle\}_{n=1,2}$ and $\{|E_n\rangle\}_{n=1,2}$, respectively. In the LZ model (see Fig. 2.1), the diabatic energy levels (dashed lines) cross at $t = 0$, while due to the coupling Δ the adiabatic potential curves (solid lines) avoid the crossing, with the minimal separation being Δ at the origin. Therefore, Δ is also called the (minimal) *level splitting* or *energy gap*. Also note how the adiabatic states change their characteristics: While for $t \rightarrow -\infty$ the two states $|1\rangle$ and $|E_1\rangle$ coincide, for $t \rightarrow +\infty$ the two states $|2\rangle$ and $|E_1\rangle$ share the same eigenvalue.

In order to study the dynamic behaviour of the system at an ACs, we define the probability of non-adiabatic transition at given time instant by:

$$\mathcal{P}(t) = 1 - |\langle E_n(t) | \Psi(t) \rangle|^2 \quad (2.22)$$

It gives the probability that the system is not in instantaneous eigenstate $|E_n(t)\rangle$ at time t . For the exactly solvable LZ model we are interested in the particular solutions that describe (adiabatic) population transport along the crossing. Therefore we demand that the initial state to be the ground state $|E_0(t)\rangle$ long before the crossing (ideally for $t \rightarrow -\infty$) and we consider the probability of non-adiabatic transitions long after the crossing (for $t \rightarrow \infty$). In this asymptotic limit the probability of

non-adiabatic transition is given by the *Landau-Zener formula*

$$\mathcal{P}_{LZ} = \exp\left\{-\pi \frac{\Delta^2}{2\alpha}\right\}. \quad (2.23)$$

At detailed derivation is given in Appx. A.

This famous formula is the main result of the LZ model. It gives the survival probability of a non-adiabatic transition scenario in the two-level case. Further, it only depends on two parameters: the coupling Δ and the sweep rate α . Alternatively, the AC can be characterized by the *interaction time* $\tau_0 = \Delta/\alpha$. Because of this simplicity, it is usually used to model single AC events embedded in more complex spectra.

Possible Generalization An intuitive generalization is given by adding linear diabatic potential lines to the spectrum. Thereby, the Hamiltonian constituting an N -level quantum system can be constructed as

$$H_{ii}(t) = \epsilon_i + \alpha_i t \quad \text{and} \quad H_{ij} = V_{ij} \quad \text{for} \quad i \neq j, \quad (2.24)$$

where ϵ_i and α_i are energy bias and slope of the i -th diabatic state and V_{ij} is the real coupling element between respective diabates. Moreover, the indices are chosen such that the slopes $\alpha_i \in \mathbb{R}$ are ordered, i.e., $\alpha_i < \alpha_j$ for $i < j$. In this special case there are analytical solutions and a generalized LZ formula can be derived for arbitrarily many linear time-dependent levels. As stated and proven by [Volkov and Ostrovsky \(2004\)](#) the survival probability of the initially populated diabatic state is

$$\mathcal{P} = \exp\left\{-2\pi \sum_{j \neq 1}^N \frac{V_{1j} V_{j1}}{|\alpha_1 - \alpha_j|}\right\} \quad (2.25)$$

provided α_1 is the largest (or smallest) of all slopes. The later is import as to ensure that the population lost at each crossing cannot return at a later transition, i.e., no destructive interference (feedback) is allowed.

2.3 Control Theory: Transitionless Quantum Driving

The idea of TQD theory was developed by [Berry \(2009\)](#) and [Demirplak and Rice \(2003\)](#) and is briefly presented in the following. Intuitively, it describes a control protocol that ensures adiabaticity of the system's dynamics by destructive interference. Let $H(t)$ be an arbitrary time-dependent Hamiltonian with instantaneous eigenstates $|E_n(t)\rangle$ and energies $E_n(t)$:

$$H(t) |E_n(t)\rangle = E_n(t) |E_n(t)\rangle. \quad (2.26)$$

In the adiabatic approximation (evolving the instantaneous eigenstates $|E_n(t)\rangle$ according to a *slowly* time-dependent Hamiltonian), the propagated states would be

$$|\Psi_n(t)\rangle = \exp \left\{ -\frac{i}{\hbar} \int_0^t dt' E_n(t') - \int_0^t dt' \langle E_n(t') | \partial_{t'} E_n(t') \rangle \right\} |E_n(t)\rangle. \quad (2.27)$$

The general expression above includes the *dynamic phase factor* as well as *geometric phase* generated by the effective vector potential $\langle E_n(t) | \partial_t E_n(t) \rangle$.

Next, we want to construct a control Hamiltonian $H'(t)$ such that $H(t) + H'(t)$ drives the eigenstates of $H(t)$ exactly, i.e., without generating transitions between them (for all values of slowness). This type of *reverse engineering* is formally characterized by the condition that

$$i\hbar \partial_t |\Psi_n(t)\rangle = (H(t) + H'(t)) |\Psi_n(t)\rangle \quad (2.28)$$

for all times.

Berry (2009) showed that for non-degenerate spectra there is exactly one choice to construct this *super-adiabatic* control Hamiltonian, as he calls it, and that it solely depends on the time derivative and the instantaneous properties of $H(t)$. The formula he derived is:

$$H'(t) = i\hbar \sum_{m \neq n} \sum_n \frac{|E_m\rangle \langle E_m | \partial_t H | E_n\rangle \langle E_n|}{E_n - E_m}, \quad (2.29)$$

where we omitted the explicit time dependence of all quantities for brevity.

An equivalent form is found by Demirplak and Rice (2003). Let $U(t)$ be the unitary transformation that changes from some static basis \mathcal{S} to the basis of instantaneous eigenstates $\mathcal{D} = \{|E_n(t)\rangle\}$ at time instance t . Then $H^{\mathcal{D}}(t) = U(t)H^{\mathcal{S}}(t)U^\dagger(t)$ is diagonal, with rows of $U(t)$ consist of eigenvectors of $H^{\mathcal{S}}(t)$. Then the *counter-diabatic* control Hamiltonian, as they call it, at time instance t is given by

$$H'(t) = i\hbar \frac{\partial U^\dagger(t)}{\partial t} U(t). \quad (2.30)$$

Further, we can check whether the adiabatic approximation is valid if

$$\left| U(t) \frac{\partial U^\dagger(t)}{\partial t} \right|_{ij} \ll \frac{1}{\hbar} |E_i(t) - E_j(t)|. \quad (2.31)$$

If not, the time-evolution of a system introduces some non-adiabaticity which has to be accounted for by the control Hamiltonian.

From now on we call the control Hamiltonian $H'(t)$ that drives the system according to TQD theory, CD Hamiltonian and denote it as $H_{CD}(t)$.

2.3.1 General Spin System

Let us derive the CD Hamiltonian for spin systems in which the spin dynamics are driven by a classical magnetic field $\mathbf{B}(t)$ of time-dependent strength $B(t) = |\mathbf{B}(t)|$ and orientation $\hat{\mathbf{n}}(t) = \mathbf{B}(t)/B(t)$. These magnetic systems will become relevant in the discussion of possible experimental realizations in Sec. 5.1. Also it nicely illustrate the construction of CD fields and includes the LZ model for later convenience.

The Hamiltonian for a general spin system takes the form

$$H(t) = \gamma \mathbf{B}(t) \cdot \mathbf{S}. \quad (2.32)$$

Here, γ is the gyromagnetic ratio, and $\mathbf{S} = (S_x, S_y, S_z)$ the vector spin operator for an arbitrary spin s . The individual spin operators obey the commutator relation

$$[S_i, S_j] = i\varepsilon_{ijk} S_k \quad (2.33)$$

and therefore the spin dynamics are governed by the special unitary group SU(2).

The super-adiabatic correction can then be calculated from Eq. (2.29) to yield

$$H_{CD} = i\hbar\gamma\partial_t\mathbf{B} \cdot \sum_{m \neq n} \sum_n \frac{|E_m\rangle \langle E_m|\mathbf{S}|E_n\rangle \langle E_n|}{E_n - E_m}, \quad (2.34)$$

where the energies are given by

$$E_n(t) = \gamma\hbar n B(t). \quad (2.35)$$

As shown by [Berry \(2009\)](#), the expression can be simplified using the fact that most matrix elements vanish. The result is

$$H_{CD} = \frac{1}{B^2} (\mathbf{B} \times \partial_t \mathbf{B}) \cdot \mathbf{S}. \quad (2.36)$$

Note how the control Hamiltonian only depends on the orientation of the vector field $\hat{\mathbf{n}}(t)$ by virtue of the cross product and is in particular independent of system specifications incorporated in γ . Thus the full Hamiltonian can be written as

$$\begin{aligned} H(t) + H_{CD}(t) &= [\gamma \mathbf{B}(t) + \hat{\mathbf{n}}(t) \times \partial_t \hat{\mathbf{n}}(t)] \cdot \mathbf{S} \\ &= \gamma \tilde{\mathbf{B}}(t) \cdot \mathbf{S}. \end{aligned} \quad (2.37)$$

For arbitrary $\mathbf{B}(t)$, the modified magnetic field

$$\tilde{\mathbf{B}}(t) = \mathbf{B}(t) + \frac{1}{\gamma} \hat{\mathbf{n}}(t) \times \partial_t \hat{\mathbf{n}}(t) \quad (2.38)$$

drives the spin evolution exactly, i.e., transitionless and non-precessing.

Now, assume that the direction $\hat{\mathbf{n}}$ of the magnetic field is parameterized as in Eq. (2.14) by the polar and azimuthal angles θ and ϕ . For the application of scheme outlined above, we then calculate

$$\hat{\mathbf{n}}(t) \times \partial_t \hat{\mathbf{n}}(t) = \partial_t \theta(t) \begin{pmatrix} -\sin \phi \\ \cos \phi \\ 0 \end{pmatrix} + \partial_t \phi(t) \begin{pmatrix} -\sin \theta \cos \theta \cos \phi \\ \sin \theta \cos \theta \sin \phi \\ \sin^2 \theta \end{pmatrix}. \quad (2.39)$$

This quantity has two contributions given by the respective time dependencies of the angles $\theta(t)$ and $\phi(t)$. Typically, we regard the spin system in the case where the external magnetic field is non-rotating, i.e., if ϕ is time-independent. We are then able to transform into a frame in which $\phi \equiv 0$ without changing the dynamics and the control Hamiltonian for a system of arbitrary spin is

$$H_{CD}(t) = \partial_t \theta(t) S_y. \quad (2.40)$$

We recognize that $\partial_t \theta(t)$ determines the shape of the control functions (elements of H_{CD}).

Landau-Zener Control For the two-state system the vector spin operator is

$$\mathbf{S} = \frac{1}{2} \boldsymbol{\sigma} \quad (2.41)$$

As described in section 2.2.1, in the LZ scenario the coupling Δ is time-independent and real. This condition translates into $\phi \equiv 0$ by virtue of Eq. (2.20). With the phase being fixed the only free parameter is the angle $\theta_{LZ}(t)$ defined by $\tan \theta_{LZ}(t) = \Delta/(\alpha t)$. Application of (2.40) gives the CD control field

$$H_{CD}(t) = \frac{1}{2} \partial_t \theta_{LZ}(t) \sigma_y \quad (2.42)$$

where

$$\partial_t \theta_{LZ}(t) = -\frac{\Delta/\alpha}{t^2 + (\Delta/\alpha)^2}. \quad (2.43)$$

Therefore the control functions for the LZ model form Lorentzian pulses. This result has major implications for the later studies on separability of control protocols discussed in Chap. 3 and Chap. 5. On the one hand we note that the control pulse is centered around the AC at $t = 0$ and has a width of $\tau_0 = \Delta/\alpha$. This motivates the idea to construct sequential control protocols for few-level systems by treating each AC as an individual event. On the other hand the tails of the Lorentzian function scale as power laws and this asymptotic behaviour for $t \rightarrow \pm\infty$ prohibits the definition of a natural scale at which the control pulse interacts with the system. This is bad for the separability as it ultimately suggests that we cannot see ACs

as phenomena which are *local* in time. Finally note, that the intensity of the peak (area underneath the signal) is finite, as is shown by explicit time integration

$$\int_{-\infty}^{+\infty} \partial_t \theta_{LZ}(t) dt = \pi. \quad (2.44)$$

In this sense we say that $\partial_t \theta_{LZ}$ constitutes a π -pulse.

3 Modelling a Three-State System

With knowledge of the LZ problem and TQD theory in mind let us advance to the more general three-level case. In accordance with our goal to study the separability of CD protocols, we present a particular three-state system whose spectrum features three avoided crossings (ACs) that are reasonably separated in time and locally resemble LZ interactions. Special cases in which the CD Hamiltonian can be derived analytically are discussed, while the full control problem is attacked numerically and by perturbation theory.

Let us motivate the model that we will be studying in this chapter. Analysis of the LZ problem shows that the probability of non-adiabaticity is extremely enhanced in the presence of an AC. As is clear by the discussion in the end of the last chapter, the SA protocol effectively suppresses these transitions via the correction term H_{CD} . Its individual control elements are Lorentzian pulses located at the AC. This suggests that we may control more complex systems with multiple isolated ACs in their spectrum by summing local correction terms. The “sequential control” protocol constructed in this way should approximately drive a system’s instantaneous eigenstates.

To grasp the notion of separability for few-level quantum systems we demand the following features:

1. The time-dependent spectrum should include at least one eigenstate that undergoes two sequential ACs.
2. These ACs should be well separated in order to be describable by effective two-level LZ interactions.

3.1 Time-Symmetric Version

We now construct an explicit model that is as simple as possible while satisfying the above mentioned requirements. Therefore we demand the diabatic potential curves to depend linearly on time as in the original LZ model and introduce an energy bias ϵ so that the crossings of the diabates are separated. Our generalized LZ scenario involving three levels is then modelled by the Hamiltonian

$$H(t) = \begin{pmatrix} \epsilon + \alpha t & \Delta/\sqrt{2} & 0 \\ \Delta/\sqrt{2} & 0 & \Delta/\sqrt{2} \\ 0 & \Delta/\sqrt{2} & \epsilon - \alpha t \end{pmatrix}. \quad (3.1)$$

That the requirements are met can be seen by regarding the instantaneous energy spectrum as a function of time as displayed in Fig. 3.1. As can be seen the spectrum features three ACs, which are characterized by the interaction of diabatic states. We call ACs that arise from explicit coupling of diabates ($H_{ij} \neq 0$) “direct”, otherwise “indirect” ($H_{ij} = 0$). Thus, our Hamiltonian models a time-symmetric system with two direct ACs at $t = \pm\epsilon/\alpha$ and one indirect AC at $t = 0$. The separation between the direct ACs is controlled via the energy offset ϵ . The indirect AC arises from the

coupling of the diabates $|1\rangle$ and $|3\rangle$ via the intermediate state $|2\rangle$. In this sense it is a second order interaction process.

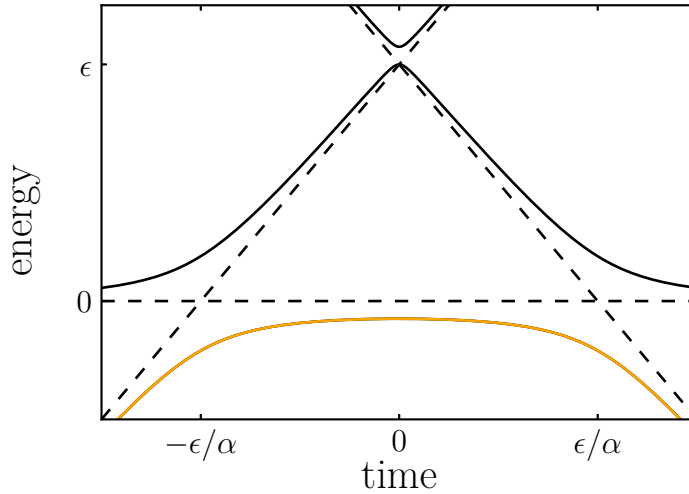


Figure 3.1: Schematic of the time-dependent spectrum of $H(t)$. Dashed and solid lines represent diabatic and adiabatic eigenstates, respectively. The temporal evolution of the ground state subject to superadiabatic control is given by the orange line.

Throughout this work the Hamiltonian and its parameters are considered to be dimensionless. This has the advantage that we do not have to worry about units and can concentrate on conceptual ideas. An explicit, dimensionfull version of $H(t)$ can always be constructed by adjusting the parameters according to some characteristic energy E_{char} of the physical system at hand. For example, dimensionless time t acquires units by letting $t \rightarrow \hbar t / E_{\text{char}}$.

3.2 Counterdiabatic Control Hamiltonian

We next want to compute the SA protocol that drives the dynamics of $H(t)$ transitionlessly. Straight-forward calculation of the CD Hamiltonian $H_{CD}(t)$ requires knowledge of the instantaneous eigenstates of $H(t)$, as is evident by Eq.(2.29). For three-level systems the general expressions involve Cardano's *casus irreducibilis*. However, these are difficult to handle especially because of their inavoidably complex-valued representation. For this reason we choose a different route and rather solve limiting cases analytically while attacking the full problem numerically. We then approximate the control pulses by perturbation theory and discuss the asymptotic scaling behaviour.

3.2.1 Analytically Solvable Limits

There are two special cases in which the CD control Hamiltonian is accessible by analytic means.

Case 1: Spin-1 System As discussed in Sec. 2.3.1, we can directly solve for the CD fields if $H(t)$ can be written as a linear combination of the respective spin operators $\{S_i\}_{i=x,y,z}$. For a spin-1 system with three internal spin degrees of freedom the respective operators are:

$$S_x = \frac{1}{\sqrt{2}} \begin{pmatrix} 0 & 1 & 0 \\ 1 & 0 & 1 \\ 0 & 1 & 0 \end{pmatrix}, \quad S_y = \frac{1}{\sqrt{2}} \begin{pmatrix} 0 & -i & 0 \\ i & 0 & -i \\ 0 & i & 0 \end{pmatrix}, \quad S_z = \begin{pmatrix} 1 & 0 & 0 \\ 0 & 0 & 0 \\ 0 & 0 & -1 \end{pmatrix}. \quad (3.2)$$

Rewriting the Hamiltonian in terms of these operators gives

$$H(t) = \epsilon S_z^2 + \alpha t S_z + \Delta S_x. \quad (3.3)$$

We now see, that for $\epsilon \equiv 0$ the TQC theory for this specific problem is identical to that of the LZ model, and the CD Hamiltonian in the diabatic basis is readily written as

$$H_{CD}(t) = \frac{\partial \theta_{Spin}(t)}{\partial t} S_y. \quad (3.4)$$

with the angle $\theta_{Spin}(t)$ defined by $\tan \theta_{Spin}(t) = \Delta/(\alpha t)$. In particular the control pulse $\partial_t \theta_{Spin}(t)$ has the same properties as $\partial_t \theta_{LZ}(t)$ from Eq. (2.43). Note, however, that for $\epsilon = 0$ all diabatic curves cross at the origin $t = 0$ and the spectrum does not feature sequential crossings. Therefore this special case is not suited for application of our sequential control protocol.

Case 2: Time Instance of the Indirect AC At the instant $t = 0$ the CD Hamiltonian can be derived for a generic $\epsilon \geq 0$. Essentially, this is due to the fact that the diabatic potential curves cross in an indirect AC event. In particular, the eigenenergies (labeled by increasing energy) at this indirect AC are exactly given by

$$E_2(0) = \epsilon, \quad E_{3,1}(0) = \frac{1}{2} \left(\epsilon \pm \sqrt{(2\Delta)^2 + \epsilon^2} \right). \quad (3.5)$$

Given these we can extrapolate the minimum distance between the two higher energy levels to be

$$\tilde{\Delta} \equiv E_3(0) - E_2(0) = \frac{\epsilon}{2} \left(\sqrt{4\Delta^2/\epsilon^2 + 1} - 1 \right). \quad (3.6)$$

This suggests that the corresponding indirect AC may be locally approximated by an effective two-level LZ interaction with coupling $\tilde{\Delta}/2$. In particular, for small ratios Δ/ϵ the coupling to first order is given by $\tilde{\Delta} \simeq \Delta^2/\epsilon$.

As the explicit calculation of the $H_{CD}(t)$ is lengthy we only present the results and refer to Appx. B for the detailed derivation.

At the origin the CD Hamiltonian takes the form

$$H_{CD}(t=0) = \frac{i}{\sqrt{2}} \left. \frac{\partial \theta_{Spin}(t)}{\partial t} \right|_{t=0} \begin{pmatrix} 0 & -1 & -\sqrt{2}\epsilon/\Delta \\ 1 & 0 & -1 \\ \sqrt{2}\epsilon/\Delta & 1 & 0 \end{pmatrix} \quad (3.7)$$

where $\partial_t \theta_{Spin}(0) = \alpha/\Delta$. There are two important things to be noted. Firstly, although the direct ACs are positioned away from the origin the elements $(H_{CD}(0))_{12}$ and $(H_{CD}(0))_{23}$ are independent of ϵ and constantly given by $\alpha/(\sqrt{2}\Delta)$. Secondly, we see that the off-diagonal element $(H_{CD}(0))_{13}$ is in general non-zero and particularly proportional to ϵ .

By noting that

$$\{S_x, S_y\} = S_x S_y + S_y S_x = \begin{pmatrix} 0 & 0 & -i \\ 0 & 0 & 0 \\ i & 0 & 0 \end{pmatrix}, \quad (3.8)$$

Eq. (3.7) can equivalently be written as

$$H_{CD}(t=0) = \frac{\alpha}{\Delta} \left(S_y + \frac{\epsilon}{\Delta} \{S_x, S_y\} \right). \quad (3.9)$$

This version explicitly shows that the dynamics are no longer described by the action SU(2) but rather by the more general SU(3). This is an important issue concerning the realizability of control protocols.

Obviously, the implementation is possible if the respective matrix elements of H can be addressed externally. Regarding our problem in terms of spin operators, Eq. (3.3), we see that we can control the coupling elements H_{12} and H_{23} simultaneously via a single magnetic field B_x (B_y). However, there is no “natural” way to manipulate the elements individually. The same is true for the single coupling element H_{13} . Although $H_{CD}(t)$ can be derived theoretically, there is not necessarily an intuitive way to realize it in a physical system. It is just not clear how to implement the anti-commutator of spin operators and thereby couple the diabatic states $|1\rangle$ and $|3\rangle$.

3.2.2 Numerical Shape of Control Pulses

In order to analyse the SA protocol for arbitrary separations of the direct ACs, we compute numerically the full control Hamiltonian $H_{CD}(t)$ according to Eq. (2.29). Importantly, keep in mind that $H_{CD}(t)$ drives any of the three eigenstates exactly at the same time, although we are mainly concerned with the ground state, which undergoes two ACs.

Let us inspect the individual control elements $(H_{CD})_{ij}$. The diagonal entries vanish by construction and as the control Hamiltonian is hermitian, we can focus

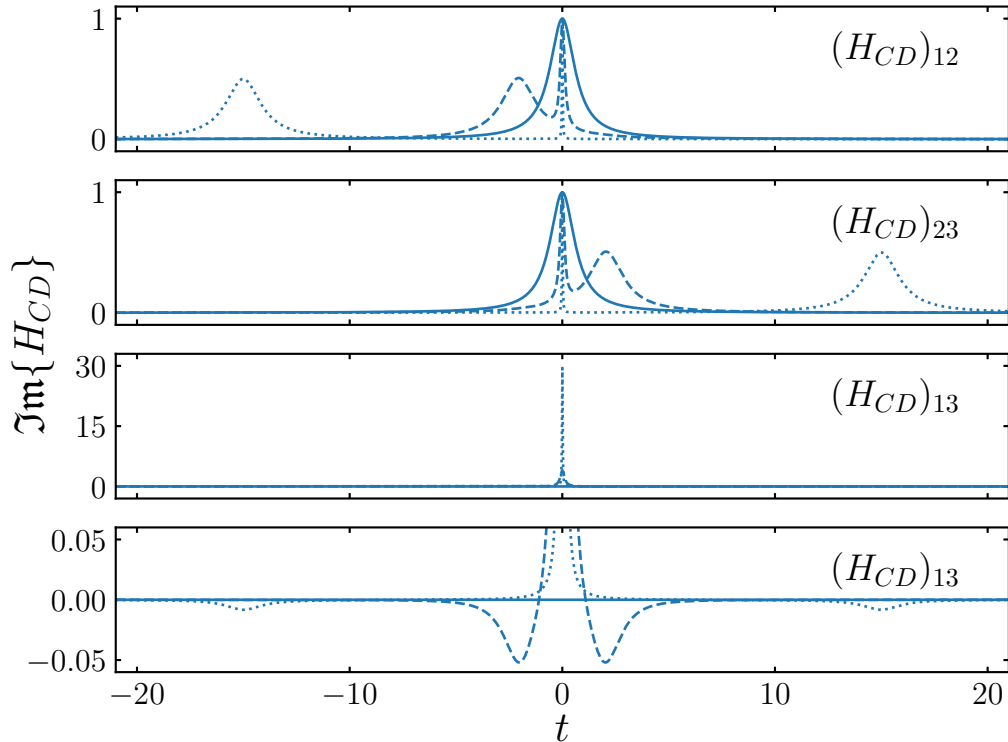


Figure 3.2: Shape of CD control elements $(H_{CD})_{12}$, $(H_{CD})_{23}$ and $(H_{CD})_{13}$ as functions of time. Solid, dashed and dotted lines correspond to separations $\epsilon = 0, 2, 15$, respectively. Parameters are: $\alpha = 1$, $\Delta = 1/\sqrt{2}$.

on the elements $(H_{CD})_{12}$, $(H_{CD})_{23}$ and $(H_{CD})_{13}$. The shape of the control elements is shown in Fig. 3.2 for different values of ϵ .

We first regard the time symmetric elements $(H_{CD})_{23}(t) = (H_{CD})_{12}(-t)$. In the analytically solvable case $\epsilon = 0$ (solid lines) the peaks are Lorentzian functions centered around $t = 0$ as is clear from Eq. (3.4). For small (dashed lines) and large (dotted lines) ϵ , the main peaks shift with respect to the origin. Their center, i.e. the position of the ACs, is approximately given by $t = \pm\epsilon/\alpha$ and their maximum reduces to half the value they have for $\epsilon = 0$. Note that a sharp peak of constant height is located at the origin for all values of ϵ as described by Eq. (3.7). As this peak is connected to indirect AC, we expect it to be negligible for the ground state dynamics.

Next we regard the remaining non-trivial element $(H_{CD})_{13}$. It is non-zero for finite separations and similar to the other elements it features a sharp peak at the origin of maximum proportional to ϵ . However, it also features negative peaks close the direct ACs whose maxima are small compared to all other peaks. The presence of those negative peaks further affirms that the SA protocol effects the entire spectrum and cannot be fully decomposed into local corrections involving only the respective crossing states.

3.2.3 Weak Coupling Limit

In order to derive approximate forms of the elements of H_{CD} , we study the full system in the limit of weak interaction, i.e., for small couplings Δ . Then, application of stationary perturbation theory as described in Appx. C gives the following profiles for the control functions:

$$(H_{CD})_{12} = i \frac{\dot{\omega}}{(\epsilon + \omega)^2} \frac{\Delta}{\sqrt{2}} + \mathcal{O}(\Delta^3), \quad (3.10a)$$

$$(H_{CD})_{23} = i \frac{\dot{\omega}}{(\epsilon - \omega)^2} \frac{\Delta}{\sqrt{2}} + \mathcal{O}(\Delta^3), \quad (3.10b)$$

$$(H_{CD})_{13} = i \frac{\dot{\omega} \epsilon (\epsilon^2 - 5\omega^2)}{4\omega^2 (\omega^2 - \epsilon^2)^2} \Delta^2 + \mathcal{O}(\Delta^3). \quad (3.10c)$$

Here, $\omega(t) = \alpha t$ is the linear time dependence of our system and $\dot{\omega}$ denotes its derivative. While the leading order for the control elements related to the direct ACs is $\sim \Delta$, the one for the control of the indirect AC is $\sim \Delta^2$. This witnesses the fact that the narrower crossing at $t = 0$ is the result of a non-adiabatic coupling acting at second-order in Δ . Perturbation theory, as is often the case, allows to reinterpret the indirect interaction in terms of an effective direct coupling, which shows up at the second order in Δ . Comparison with the exact controls (see Fig. 3.2) shows that all peaks except for the central peak of $(H_{CD})_{12}$ is accounted for.

The main difference lays in the description of the peaks which are modelled as singularities in the perturbative approach reflecting the fact that the perturbation is assumed to be small. By promoting these singularities to Lorentzians of appropriate width, we get a smooth approximate analytic expression for the controls free of singularities. For the direct ACs we choose a width of $\sqrt{2}\Delta$ with the factor of two conveniently taking into account that the crossing happens at half the speed. The width of indirect AC is estimated by Eq. (3.6). Thereby,

$$(H_{CD})_{12} = i \frac{\dot{\omega}}{2\Delta^2 + (\epsilon + \omega)^2} \frac{\Delta}{\sqrt{2}}, \quad (3.11a)$$

$$(H_{CD})_{23} = i \frac{\dot{\omega}}{2\Delta^2 + (\epsilon - \omega)^2} \frac{\Delta}{\sqrt{2}}, \quad (3.11b)$$

$$(H_{CD})_{13} = i \frac{\dot{\omega} \epsilon (\epsilon^2 - 5\omega^2) \Delta^2}{4[2\Delta^2 + (\epsilon + \omega)^2][(\frac{\Delta^2}{2\epsilon} + \omega^2)][2\Delta^2 + (\epsilon - \omega)^2]}. \quad (3.11c)$$

The elements $(H_{CD})_{12}$ and $(H_{CD})_{23}$ are Lorentz pulses centered at the direct ACs. The shape of $(H_{CD})_{13}$ is more complicated involving the product of three Lorentzians. This is necessary to include the positive as well as negative peaks (see Fig. 3.2).

3.2.4 Asymptotic Behaviour

Let us now focus on the asymptotic behaviour of the control functions. In order to obtain expressions reflecting the long-time behaviour of $H_{CD}(t)$ we again consult

perturbation theory. However, this time we expand around the asymptotic limit $t \rightarrow \infty$. This is done by considering the rescaled version $H(t)/t$ which shares the instantaneous eigenstates with the original $H(t)$. The explicit calculations are done in Appx. C giving the $1/t$ -leading terms of the control functions. The resulting behaviour of the asymptotic tails far from ACs is

$$H_{CD}(t \rightarrow \infty) \propto i \begin{pmatrix} 0 & \Delta t^{-2} & -\Delta^2 t^{-4} \\ -\Delta t^{-2} & 0 & \Delta t^{-2} \\ \Delta^2 t^{-4} & -\Delta t^{-2} & 0 \end{pmatrix}. \quad (3.12)$$

We now see that all elements scale as power laws in the asymptotic limit. These findings are indeed verified by numerical evaluation as shown in Fig. 3.3. Note, how the scaling of $(H_{CD})_{13}$ (dotted line) for small times is proportional to t^{-2} until it switches sign at $t = \epsilon/(\sqrt{5}\alpha)$ (singularity in the plot). Finally, after the direct AC at ϵ/α the tail scales as t^{-4} . Actually, terms of order t^{-3} also appear in the perturbative calculation for the indirect AC, but they cancel each other exactly due to the temporal symmetry of the problem. The exact cancellation no more happens when such symmetry is broken. this feature will be discussed in the next section.

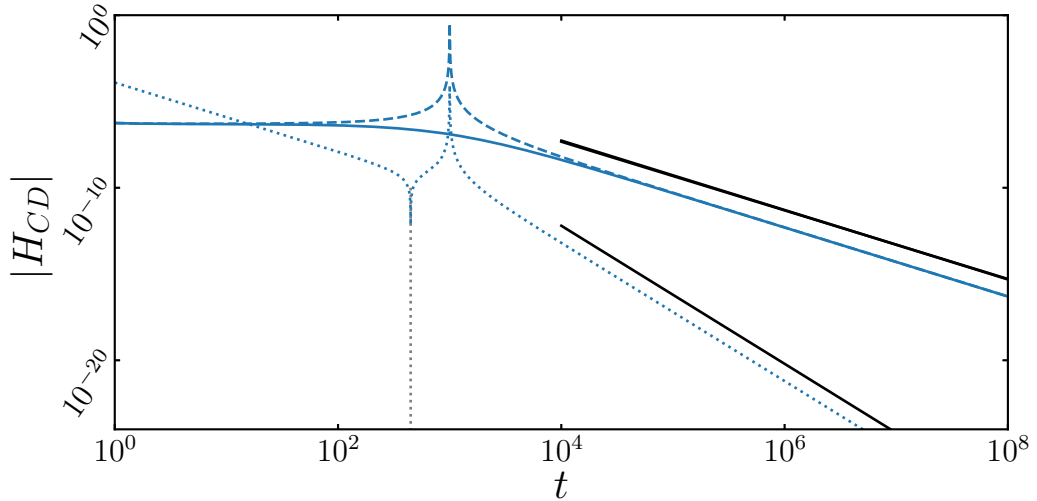


Figure 3.3: Asymptotic (large t) behaviour of control elements for $\epsilon = 1000$. Full, dashed and dotted lines are used for the elements $(H_{CD})_{12}$, $(H_{CD})_{23}$ and $(H_{CD})_{13}$, respectively. The power law fits (black lines) are shifted for better visibility. The respective fit coefficients are -2 , -2 and -4 . Parameters are $\alpha = 1$, $\Delta = 0.5$.

3.3 Time-Asymmetric Version

In this section we present a second generalization of the LZ problem by allowing for asymmetric spectra. In this variant the left and right ACs are no longer equal in

terms of coupling strength and sweep constant. We discuss how this changes the asymptotic behaviour of the control pulses and the consequences for the robustness of the SA protocol.

The general Hamiltonian in this scenario is given by

$$H(t) = \begin{pmatrix} \epsilon + \alpha t & \Delta_1 & 0 \\ \Delta_1 & 0 & \Delta_2 \\ 0 & \Delta_2 & \epsilon - \beta t \end{pmatrix}. \quad (3.13)$$

From this definition we see that two types of asymmetry are introduced. The first one effects the general form of the spectrum: the “isoscele” triangular configuration is broken since the slopes of the two diabatic potential curves are independently given by $\alpha, \beta > 0$. The second one distinguishes the left and right ACs by the separately tunable coupling elements Δ_1 and Δ_2 . Figure 3.4 displays the new temporal evolution of the instantaneous energy spectrum for a representative parameter configuration. Comparison with the symmetric version (Fig. 3.1) indicates that two direct ACs are still positioned to the left and right of the origin but now crossing the horizontal curve at $t = -\epsilon/\alpha$ and $t = \epsilon/\beta$, respectively. Also, in contrary to the symmetric case the indirect AC is shifted with respect to the origin. Clearly, the requirements for potential sequential control protocols, which we mentioned in the beginning of this chapter, are fulfilled for large separations of ACs and respective small couplings. Moreover note that the symmetric version is included by setting $\Delta_1 = \Delta_2 = \Delta/\sqrt{2}$ and $\alpha = \beta$.

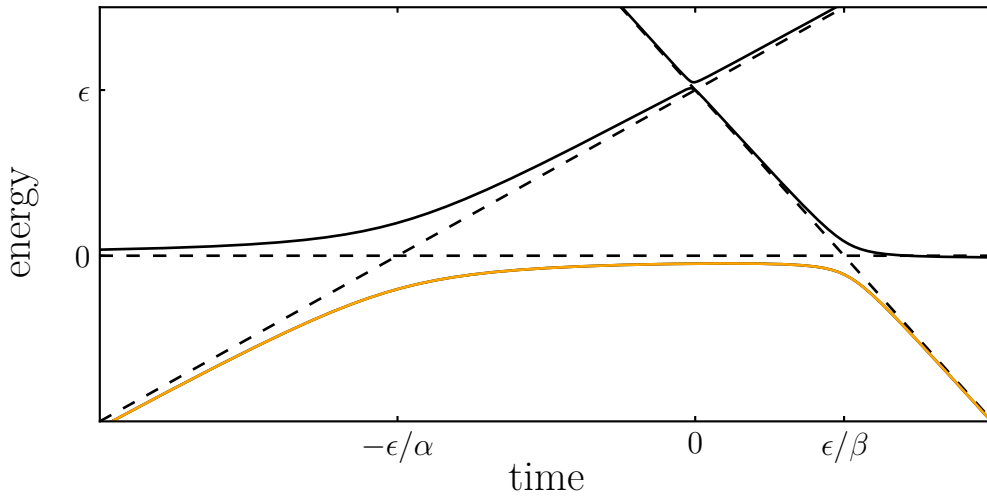


Figure 3.4: Schematic of the time-dependent spectrum of $H(t)$. Dashed and solid lines represent diabatic and adiabatic eigenstates, respectively. The temporal evolution of the ground state subject to superadiabatic control is given by the orange line. The specific configuration of parameters is $\alpha = \Delta_2 = 1$, $\beta = \Delta_1 = 2$, $\epsilon = 10$.

Let us next regard the asymptotic behaviour of the new control pulses. Repeating the perturbative analysis we calculate the CD Hamiltonian for $t \rightarrow \infty$. The results

differ only in $(H_{CD})_{13}$ from the symmetric case, which is given by

$$(H_{CD})_{13} = \frac{i\Delta_1\Delta_2(\alpha - \beta)}{\alpha\beta(\alpha + \beta)t^3} - \frac{i\Delta_1\Delta_2\epsilon(2\alpha^2 + 2\beta^2 + \alpha\beta)}{\alpha^2\beta^2(\alpha + \beta)t^4} + \mathcal{O}(t^{-5}) \quad (3.14)$$

We see that the asymmetry introduces a t^{-3} term, which as is the nature of power law scalings, will always dominate the large time scaling behaviour of the tails. The transition time t_c at which the tail changes its dominating time-dependency from t^{-4} to t^{-3} can be estimated by equating the competing terms. Rearrangement and subsequent cancellation yields

$$\begin{aligned} t_c &= \frac{2\alpha^2 + 2\beta^2 + \alpha\beta}{\alpha\beta(\alpha - \beta)}\epsilon \\ &= \frac{2(\alpha - \beta)\epsilon}{\alpha\beta} + \frac{5\epsilon}{\alpha - \beta}, \end{aligned} \quad (3.15)$$

where we completed the square to arrive at the later form. For small variations $\delta = |\alpha - \beta| \ll 1$ the first term can be neglected and the transition point is

$$t_c \simeq \frac{5\epsilon}{\delta}. \quad (3.16)$$

In the totally symmetric case where $\alpha = \beta$ ($\delta = 0$), the t^{-3} in the perturbative expansion (3.14) vanishes and consequently $t_c \rightarrow \infty$. Moreover, asymmetries in the couplings of the left and right ACs leave the scaling of the asymptotic tails unaffected. This is reasonable as variations in the interaction strength increase the splitting of the adiabatic curves at the AC while keeping its position.

3.3.1 Sequential Control Hamiltonian

We now want to approximate the exact control by local correction terms. The general strategy is that each time the system undergoes an AC, a superadiabatic two-level control pulse is applied in order to drive the system transitionlessly. In particular, each crossing is treated as an independent LZ event. We focus on driving the instantaneous ground state of our system through the two sequential LZ crossings it passes ignoring the third anti-crossing between the other states. We thereby call this procedure the sequential control (SC) scenario.

In order to define the SC Hamiltonians, let us introduce the matrices $U_L(t)$ and $U_R(t)$ which diagonalize respectively the upper-left and lower-right two-by-two submatrices of $H(t)$. They transform in a local eigenbasis at the left (L) and right (R) ACs. From Eq. (2.16), they are defined by

$$U_L(t) = \begin{pmatrix} \cos \frac{\theta_L(t)}{2} & \sin \frac{\theta_L(t)}{2} & 0 \\ \sin \frac{\theta_L(t)}{2} & -\cos \frac{\theta_L(t)}{2} & 0 \\ 0 & 0 & 1 \end{pmatrix}, \quad (3.17a)$$

$$U_R(t) = \begin{pmatrix} 1 & 0 & 0 \\ 0 & \cos \frac{\theta_R(t)}{2} & \sin \frac{\theta_R(t)}{2} \\ 0 & \sin \frac{\theta_R(t)}{2} & -\cos \frac{\theta_R(t)}{2} \end{pmatrix} \quad (3.17b)$$

with the angles being defined by

$$\tan \theta_L(t) = \frac{2\Delta_1}{\alpha t + \epsilon} \quad \text{and} \quad \tan \theta_R(t) = \frac{2\Delta_2}{\beta t - \epsilon}. \quad (3.18)$$

With these local transformation matrices at hand we now give two definitions of the SC Hamiltonian, an *ideal* and a *realizable* version.

The ideal one is constructed from the individual corrections of the (L) and (R) ACs according to the definition of the CD fields in Eq. (2.30). It takes the form.

$$\begin{aligned} H_{\text{ideal}}(t) &= i \frac{\partial U_L^\dagger}{\partial t} U_L + i \frac{\partial U_R^\dagger}{\partial t} U_R \\ &= \frac{i}{2} \begin{pmatrix} 0 & -\partial_t \theta_L(t) & 0 \\ \partial_t \theta_L(t) & 0 & -\partial_t \theta_R(t) \\ 0 & \partial_t \theta_R(t) & 0 \end{pmatrix}. \end{aligned} \quad (3.19)$$

Comparison with the perturbative results (3.11) shows that H_{ideal} is exactly H_{CD} to first order in Δ and after promotion of the singularities to Lorentzians. From a conceptual point of view, this is no surprise since we intentionally corrected the direct ACs and ignored the indirect one. Thereby, it constitutes the simplest valid SC Hamiltonian and is ideal in the sense that it only features CD peaks where needed.

However, this minimal choice of SC Hamiltonian does not admit a simple decomposition in terms of spin-1 operators. As a consequence the experimental implementation is not obvious. In order to overcome this issue, we present a second choice of SC Hamiltonian which focuses on experimental realizability:

$$H_{\text{real}}(t) = i \partial_t \theta_{\text{real}} S_y. \quad (3.20)$$

Here, the shape of the control pulse is given by summing the contributions of the single (L) and (R) crossing corrections

$$\begin{aligned} \partial_t \theta_{\text{real}} &= \partial_t \theta_L(t) + \partial_t \theta_R(t) \\ &= -\frac{2\alpha\Delta_1}{(\epsilon + \alpha t)^2 + (2\Delta_1)^2} - \frac{2\beta\Delta_2}{(\epsilon - \beta t)^2 + (2\Delta_2)^2}. \end{aligned} \quad (3.21)$$

The control functions $(H_{\text{real}})_{12}$ and $(H_{\text{real}})_{23}$ now feature two peaks, one at each direct AC. This is justified as the peak of $(H_{\text{real}})_{12}$ at the (R) AC does not induce transition between the respective diabates. Formally, the peak is negligible if the intensity of the control pulse is small compared to the separation of energy levels, compare Eq. (2.31). At the (R) AC this condition is approximately given by

$$|\partial_t \theta_R(\epsilon/\alpha)| = \frac{\alpha}{\sqrt{2}\Delta} \ll \alpha\epsilon, \quad (3.22)$$

which is valid for large ϵ .

4 Ground State Dynamics

In the last chapter we analysed the exact CD fields for the specific Hamiltonian, Eq. (3.13), and obtained approximate analytic expressions by perturbation theory. We then discussed the possibility of separating the protocol into local corrections. We now want to regard the effects of exact SA and approximate SC protocols on the dynamics of the system, where we focus on adiabatic following of the ground state. This is motivated by the fact that many quantum control problems require adiabatic control over exactly one of the instantaneous eigenstates. This is true especially in multi-level spectra where the number of ACs is very large, although the evolution of only one instantaneous eigenstate is of interest.

4.1 Numerical Details

In order to study the dynamics we integrate the time-dependent Schrödinger equation numerically (2.5). We work in *python* and use the integration routines *zvode* and *dop853* provided by *scipy.integrate.ode*¹. The *zvode* algorithm directly integrates the set of N -complex ordinary differential equations by an implicit Adams method for time efficiency. This linear multi-step method gains its speed up by including previous evaluations into the calculation at the current iteration step. Contrarily, *dop853* is an explicit Runge-Kutta method and thereby an intermediate step approach whose order is independent of previous results and adjusted at each step (either 8,5 or 3). As such this method focuses on precision and is especially useful in studying of asymptotic probabilities. Further, both algorithms are implemented using internally adaptive step size. This is especially important for cases where the temporal changes in the Hamiltonian are large.

For our numerical studies we use the following procedure. We begin by preparing the system in some initial state $|\Psi_i\rangle$, which is typically the instantaneous ground state of $H(t)$ at some initial time t_i . Then we propagate the system in time using $H(t) + H'(t)$, where $H'(t)$ is the Hamiltonian constituting the control protocol of choice, until some final time t_f . We monitor the systems dynamics in terms of population numbers and relative phase. Importantly, the start and end points t_i and t_f are chosen such that the ground state passes all ACs. The numerical task is to ensure a small propagation error even for large propagation times. To this end, we ensure a total normalization error smaller than 10^{-8} for all propagation scenarios.

The efficiency of the method is quantified by how close the state driven by the control field $H'(t)$ results to be to the exact instantaneous ground state at the end of the protocol. Formally, we define the fidelity of a protocol driving the n -th instantaneous eigenstate by the probability

$$\mathcal{F}(t) = |\langle E_n(t) | \Psi(t) \rangle|^2, \quad (4.1)$$

where $|\Psi(t)\rangle$ is the propagated state. The error of the protocol is then defined as the derivation of \mathcal{F} from unity

$$\mathcal{P}(t) = 1 - \mathcal{F}(t). \quad (4.2)$$

¹<https://docs.scipy.org/doc/scipy-0.14.0/reference/generated/scipy.integrate.ode.html>

Formally, it is equal to the probability of non-adiabatic transition as defined by Eq. (2.22), although this time it is interpreted as a measure of quality for control protocols from an optimization problem point of view.

4.2 Super-Adiabatic Protocol

We first regard the effects of the SA protocol on the system. In Fig. 4.1 the temporal evolution of the system initially prepared in the ground state $|E_1\rangle$ is shown. Here, the left and right frames visualize the dynamics for the uncontrolled and CD-controlled scenarios, respectively. The main visual difference is the smoothness of the lines in the CD-controlled case compared to the oscillatory behaviour in the uncontrolled case. This discrepancy is clearly visual in the temporal development of the occupation numbers (top two figures) as well as relative phases (bottom row of Fig. 4.1) in terms of the diabatic basis states. For the occupation numbers note that the asymptotic values differ in both scenarios: while the solution under sole propagation of $H(t)$ oscillates leaving the system in a superposition of all diabates the dynamics of $H(t) + H_{CD}(t)$ are smooth and describe a complete switching of diabatic states. Further regarding the phase differences, we see that the CD protocol drives population as well as relative phases exactly.

Let us discuss this dynamic process in detail and step by step. We prepare the system in the ground state $|E_1\rangle$ at $t_i = -50$ such that mainly the diabate $|1\rangle$ is occupied. By choice of parameters the first direct AC happens at $t = -15$ after which the ground state is approximately given by $|2\rangle$. This is the point at which the two scenarios first differ: while in the CD-controlled system the population transfer is complete, the switching is incomplete in the uncontrolled system. In the later case, the syteme has a finite probability to still be in the state $|1\rangle$ after the crossing. Also the occupation numbers begin to oscillate and the the phase differences start to rotate. These effects are reminiscent of the idealized LZ-type crossing. At the origin $t = 0$ the two excited states exchange.

Advancing further in time, we next approach the indirect AC at the origin. The effect of this indirect AC on the ground state dynamics is hardly visible in the uncontrolled scenario, although it introduce small oscillations in the phase difference $\delta\phi_{13}$ between the crossing states. Indeed, the minor impact of this crossing was expected by perturbation theory in which the crossing appeared only as a second order interaction term.

At $t = +15$, the system undergoes a symmetric (R) AC but now involving the diabatic states $|2\rangle$ and $|3\rangle$. As the interaction strength is equal to the first, the population transfer and oscillation patterns are comparable. Only this time $|2\rangle$ the incoming population oscillates giving rise to a more complicated superposed oscillation pattern after the crossing. Far away from the crossing, we may take the population of $|3\rangle$ as an indicator for adiabatic population transfer since it tends towards $|E_0\rangle$ for $t \rightarrow +\infty$. In total, by virtue of $H_{CD}(t)$ the non-adiabatic effects in the dynamics are effectively suppressed and $|\Psi(t)\rangle$ and $|E_1(t)\rangle$ describe the same

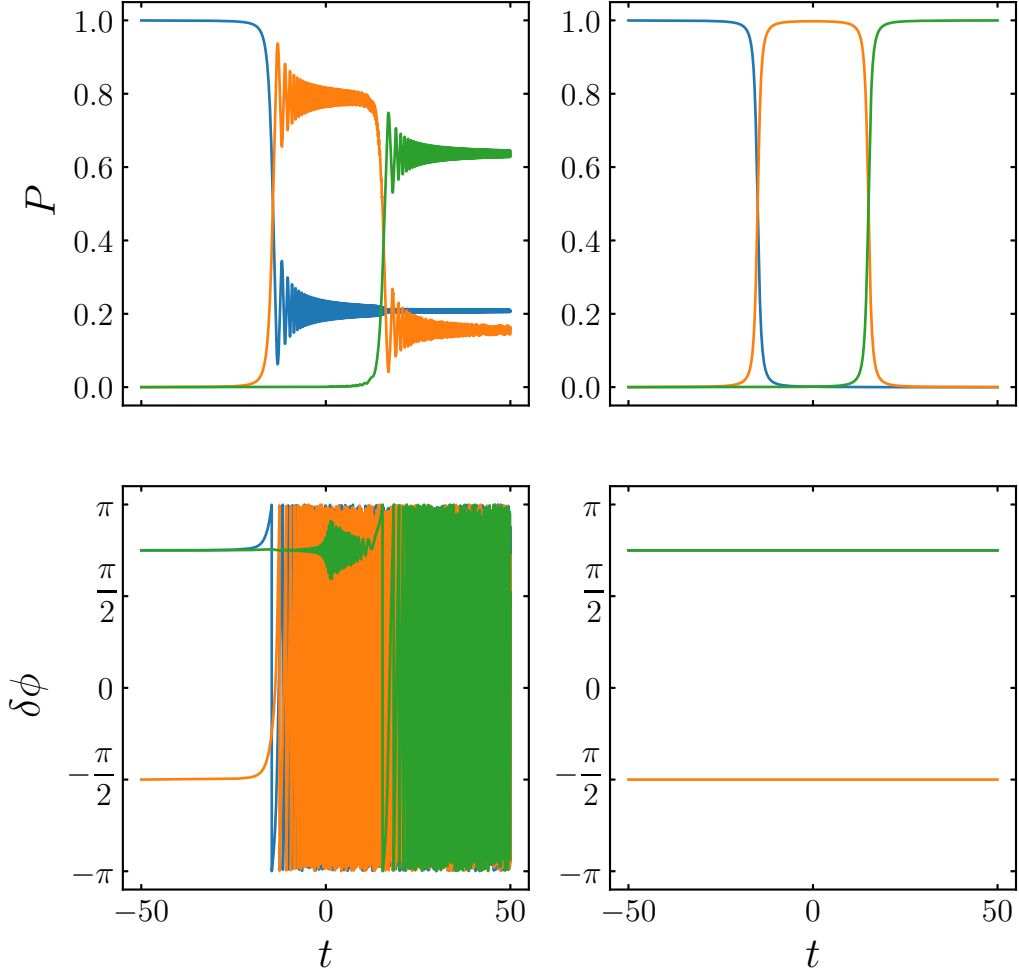


Figure 4.1: Dynamics of the uncontrolled (left) and CD-controlled system (right). The control is computed numerically according to Eq. (2.29). Blue, orange and green lines represent the population of (top row) and phase difference between (bottom row) the diabatic states $\{|n\rangle\}_{n=1,2,3}$. In both cases the initial state is taken to be the ground state $|E_1\rangle$. Parameters are: $\alpha = 1$, $\Delta = (1 + i)/(2\sqrt{2})$, $\epsilon = 15$.

state at all times as expected.

4.2.1 Robustness

The SA protocol drives the instantaneous ground state of $H(t)$ exactly provided the system starts in the ground state. Naturally, we ask what happens if the system is initially prepared in a state different than the ground state. To answer this question, note that the initial state can always be written in the adiabatic basis at t_i

$$|\Psi_i\rangle = \sum_n c_n |E_n(t_i)\rangle. \quad (4.3)$$

By construction H_{CD} drives each of these states in the adiabatic approximation as described in Sec. 2.3. Therefore, the final state can be readily written as

$$|\Psi_f\rangle = \sum_n c_n |\Psi_n(t_f)\rangle \quad (4.4)$$

$$= \sum_n c_n \exp\left\{-i \int_{t_i}^{t_f} dt E_n(t) - \int_{t_i}^{t_f} dt \langle E_n(t) | \partial_t E_n(t) \rangle\right\} |E_n(t_f)\rangle. \quad (4.5)$$

The time propagation introduces a dynamic and geometric phase to each instantaneous eigenstate. While the population of the adiabatic basis states is stationary the relative phase varies with time.

In Fig. 4.2 this behaviour is visualized by numerical time integration. Note that the relative phase angle oscillates quickly far from the ACs but takes definite values at the ACs. Rather than starting the propagation with $|E_1(t_i)\rangle$ at time t_i we now prepare the system in the diabatic state $|1\rangle$ which coincides with $|E_1(t)\rangle$ in the asymptotic limit $t \rightarrow \infty$.

By initiating propagation at finite time t_i multiple adiabatic states are populated and the error with respect to the case where the initial state is the exact instantaneous ground state is given by

$$\text{err}(t) = 1 - |\langle E_1(t) | 1 \rangle|^2. \quad (4.6)$$

This quantity can be estimated in the asymptotic time limit by substituting the perturbative result for $|E_1(t)\rangle$ given by Eq. (C.22). As the spectrum is time symmetric the error at t and $-t$ is identical and for t large, we therefore find

$$\begin{aligned} \text{err}(t) &= 1 - \left|1 - \frac{\Delta^2}{4\alpha^2 t^2}\right|^2 \\ &= 1 - \left(1 - \frac{\Delta^2}{4\alpha^2 t^2} + \frac{\Delta^4}{16\alpha^4 t^4}\right) \\ &\simeq \frac{\Delta^2}{4\alpha^2 t^2}. \end{aligned} \quad (4.7)$$

Here, in the first and last quantities, we kept only terms to the leading order in $1/t$. The preparation error far from the first AC scales as a power law $\propto t^{-2}$. This is indeed verified by a numerical calculation, see Fig. 4.3. Therefore, fixing a threshold value for the error we can read the calculate the time t_c at which deviation of diabatic and adiabatic states is given by that error according to Eq. (4.7) or vice-versa. Then, by preparing the system in the state $|1\rangle$ at $t_i = t_c$ this initial error is transported by the SA protocol for all times.

4.3 Sequential Control Protocol

Finally, let us test our SC protocol and confront it with the exact results. For simplicity, we here study the sequential control scheme (see Sec. 3.3.1) applied to

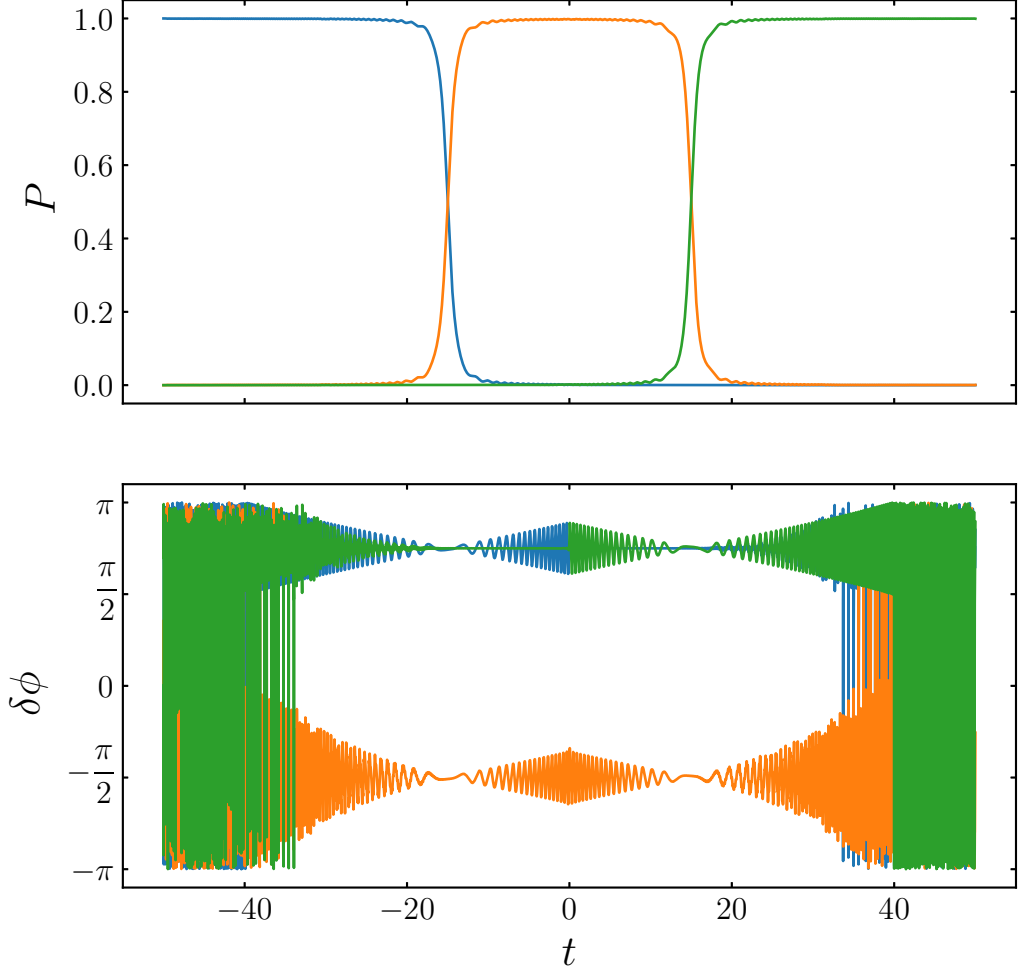


Figure 4.2: Dynamics of the CD-controlled system with the initial state $|1\rangle$. Blue, orange and green lines represent the population of (top row) and phase difference between (bottom row) the diabatic states $\{|n\rangle\}_{n=1,2,3}$. The control is computed numerically according to Eq. (2.29). Parameters are: $\alpha = 1$, $\Delta = (1 + i)/(2\sqrt{2})$, $\epsilon = 15$.

the symmetric version of our system. The ideal and realistic control Hamiltonian are then given in terms of the Lorentzians

$$\partial_t \theta_{L/R}(t) = -\frac{\sqrt{2}\alpha\Delta}{(\epsilon \pm \alpha t)^2 + 2\Delta^2}. \quad (4.8)$$

These are

$$(H_{\text{ideal}})_{12}(t) = -\frac{i}{2}\partial_t \theta_L, \quad (H_{\text{ideal}})_{23}(t) = -\frac{i}{2}\partial_t \theta_R \quad (4.9)$$

and

$$H_{\text{real}}(t) = \frac{1}{\sqrt{2}}(\partial_t \theta_L + \partial_t \theta_R)S_y. \quad (4.10)$$

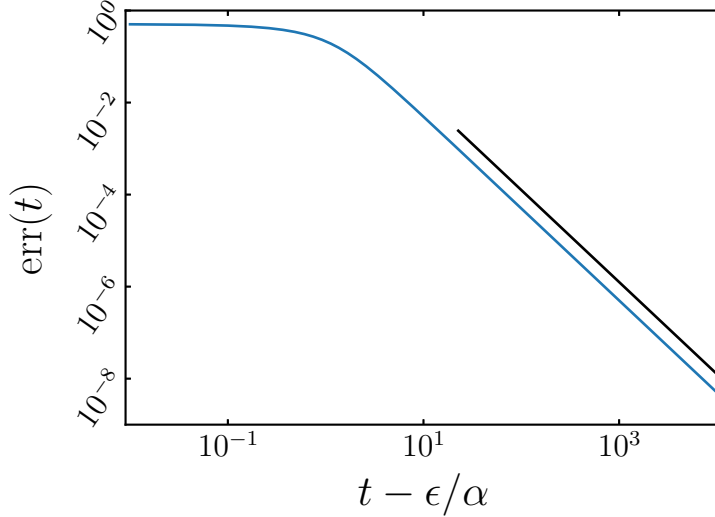


Figure 4.3: Deviation of adiabatic state $|3\rangle$ from instantaneous ground state $|E_1(t)\rangle$ in terms of population after the second ACs at ϵ/α . The signature of the power law fit is -2 . Parameters are: $\alpha = 1$, $\Delta = 1$, $\epsilon = 15$.

The dynamics as induced by the SC protocols as shown in Fig. 4.4. Here, the left and right columns display the dynamics of the ideal and realistic sequential control protocols introduced in Sec. 3.3.1, respectively. Conversely, top and bottom rows show the fidelity and the following of relative phases.

The main observation is that the ideal SC protocol yields better results than the realistic one as the probability of non-adiabaticity at the end of the protocol is about 4 times smaller. This can be explained by the additional Lorentzian in the definition of H_{real} . Because of its power law scaling it will always affect the dynamics at the other crossing. In addition, the fact that the correction is not perfect implies amplification of $\mathcal{P}(t)$ in the vicinity of the ACs. This phenomenon is present in both scenarios although much more dominant in the realizable case where additional strong oscillatory behaviour, which resembles the typical LZ transient, is observed. However, these oscillations in the population of the adiabatic ground state dampen quickly compared to the oscillations in the diabatic basis, see Fig. 4.1.

Next focusing on the relative phases, we see that after the first (L) AC, light oscillations are present involving the crossing states. They are more pronounced in the realizable scenario. After the second (R) AC the relative phases oscillate quickly denying the extraction of a definite value at the end of the protocol. We note that while SC protocols ensure approximate following of the ground state population the relative phases are intractable taking random values at the end of the protocol.

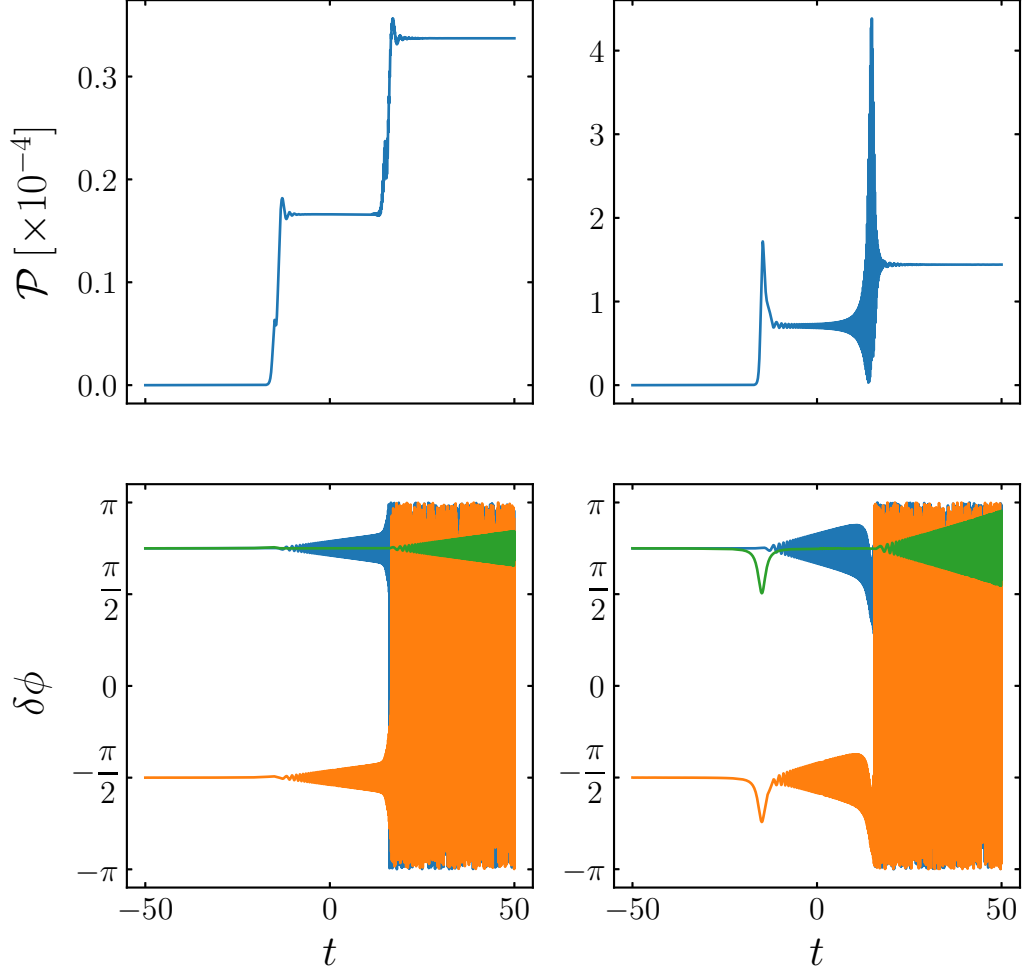


Figure 4.4: Effects of the ideal (left) and realizable (right) SC Hamiltonians on the system's dynamics. The top row shows the error of the respective protocols as defined by the probability of non-adiabaticity, Eq. (4.2). Blue, orange and green lines in the bottom row represent the phase differences $\delta\phi_{12}$, $\delta\phi_{13}$ and $\delta\phi_{23}$ between the respective expansion coefficients in the diabatic basis $\{|n\rangle\}_{n=1,2,3}$. Parameters are: $\alpha = 1$, $\Delta = (1 + i)/(2\sqrt{2})$, $\epsilon = 15$.

4.3.1 Probability of Non-Adiabaticity

The really interesting question, however, is: how does the asymptotic error $\mathcal{P}(t \rightarrow \infty)$ depend on the structure of the spectrum, in particular on the separation of ACs?

In order to study this problem repeat the SC control procedures outlined above for different values of ϵ . The initial time is chosen such that $\text{err}(t_i) = 10^{-3}$ and the system is prepared in the ground state $|E_0(t_i)\rangle$. Then after the second ACs at $t_f = -t_i$, we extract the large t error according to Eq. (4.2).

The dependency of \mathcal{P} on the separation parameter ϵ , for fixed α and Δ is shown in Fig. 4.5. The error of the ideal and realistic sequential control protocol are plotted

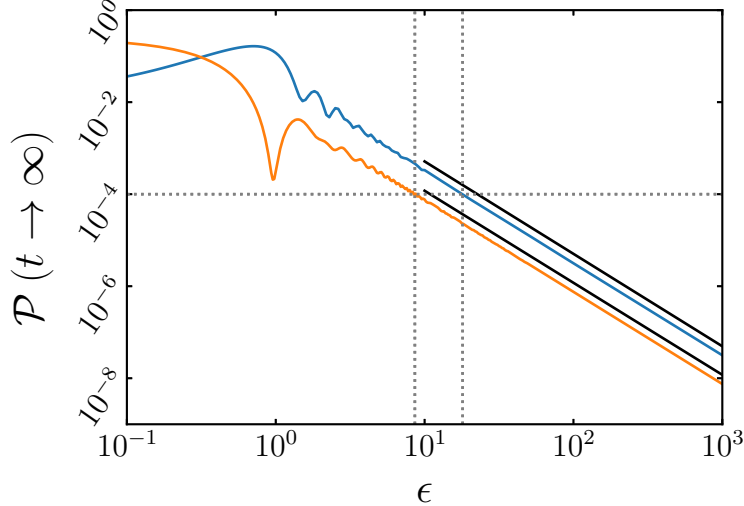


Figure 4.5: Asymptotic (large t) probability of non-adiabaticity as a function of separation parameter ϵ . Orange and blue lines correspond to ideal and realistic sequential control protocols. The power law fits for large ϵ are shifted for better visibility. The dashed lines highlight the threshold separations for $\mathcal{P} \sim 10^{-4}$. Parameters are: $\alpha = 1$, $\Delta = 0.5$.

with orange and blue lines, respectively. As a matter of fact, the realistic setup suffers from the additional peaks in the control functions, which scale as power laws and therefore effect the afidelity even for large separations. Moreover, \mathcal{P} oscillates in both cases for small ϵ .

For large ϵ , however, the oscillations in the probability are damped as the propagated states approach the exact ones, eventually following a power law as $\mathcal{P} \propto \epsilon^{-2}$. Due to the power-law scaling no natural threshold for ϵ can be defined at which the two crossings can be considered fully separable. However, given a desired fidelity one can extract the corresponding critical ϵ , or viceversa, from Fig. 4.5. As an example, for $\mathcal{P} \sim 10^{-4}$ we get $\epsilon \approx 8$ and $\epsilon \approx 18$ in the case of the ideal and realistic sequential control procedures.

Similar graphs can be produced for different values of α and Δ , all scaling with ϵ^{-2} for large separations but shifted with respect to each other. Unfortunately, no general dependency could be found.

It must be stressed that this procedure approximately drives the population of the instantaneous ground state to be close to one but does not provide a precise control on phase factors, in contrast to the exact recipe of Eq. (2.29). While the fidelity of the protocol can be chosen to be arbitrarily good by adjusting the separation parameter ϵ , the improper shape of the control pulses introduce oscillations in the relative phases.

5 Perspectives

So far we discussed our particular three-level model from the theoretical point of view and gave numerical results on the applicability of SA and SC protocols. Let us now regard possible experimental implementations and generalizations of our model.

5.1 Experimental Realization

A huge amount of temporary research is devoted to the engineering of effective two-level (qubits) and three-level (qutrits) quantum systems. In the following we will describe possible ways to realize our model in different physical setups.

Let us start by discussing magnetic systems. As is evident by Eq. (3.3) our model describes a spin-1 system, which may be realized in molecular nanomagnets (Gatteschi et al., 2006) and Nitrogen-Vacancy (N-V) color centers in diamond (Doherty et al., 2013). The term “nanomagnet” is used to describe any system at sub-micro scale which shows spontaneous magnetic order in the absence of external magnetic fields. This type of magnetization arises from internal interactions which gives rise to zero-field splitting of the spin triplet ground states. As a consequence nanomagnets are “remanent”: they remember their magnetic state and only relax slowly. Moreover, due to their mesoscopic size, nanomagnets show quantum behaviour like tunneling of magnetization and spin mixing (Carretta et al., 2004), which can be visualized in magnetic hysteresis diagrams. Usually, the physical basis for nanomagnets are artificially created nanoparticles (quantum dots) or molecules, which allow for particularly well-designed band structures of spin states. Of particular interest is the situation in which the ground state of a single-molecule magnet (SSM) is three-fold degenerate and isolated from the rest of the spectrum. Then, in the presence of magnetic fields or microwave signals this structure is effectively manipulated and energy sweeps can be realized (Zhou et al., 2017).

Two second implementation are point defects in solid-state quantum systems. Such (well-isolated) impurities in the lattice formation can have definite charge and spin quantum numbers. In the case of $N-V^-$ centers a negatively charged empty lattice site is situated next to an Nitrogen atom and two unbound electrons form an effective spin-1 system. These systems are long-lived (coherence times several μs), can be operated at room temperature and are susceptible to manipulation via time-dependent microwave pulses, magnetic and electric fields (Childress et al., 2006; Dutt et al., 2007). The advantage of solid-state systems is the long coherence time, while coupling with environment, in particular the nuclear spins of the surrounding atoms gives rise to hyperfine splittings.

Leaving the regime of magnetic substances, Bose-Einstein condensates constitute the archetype of coherent quantum systems which may be exploited for the control tasks at hand (Pitaevskii and Stringari, 2003). They are well-known to be tunable almost arbitrarily in size and interaction strength and have comparable long coherence timescales. However, due to their many-body nature the spectrum is typically complex involving large numbers of ACs. Thus the main issue is to single out specific levels and to exclusively address them. Fortunately, the isolation of effective

few-level system in optical lattices is possible as has been shown by [Bason et al. \(2012\)](#). Following their approach, we propose to load the condensate into an accelerated lattice and couple the emerging bands in sequence to generate an effective three-level system. However, due to the different band gaps leakage to higher bands is likely to occur ([Zenesini et al., 2008](#); [Tayebirad et al., 2010](#)).

Further superconducting circuits can model effective three-level systems, which then can be manipulated by microwave signals ([K. S. Kumar and Paraoanu, 2016](#)). This is the another promising route to universal quantum computation with the advantages of high versatility and scalability. A disadvantage is the typical $1/f$ noise mainly due to material defects which constitute competing two-level systems.

5.2 Four-Level System

Let us quickly show that the generalization of the sequential control protocol to a four-level system is possible.

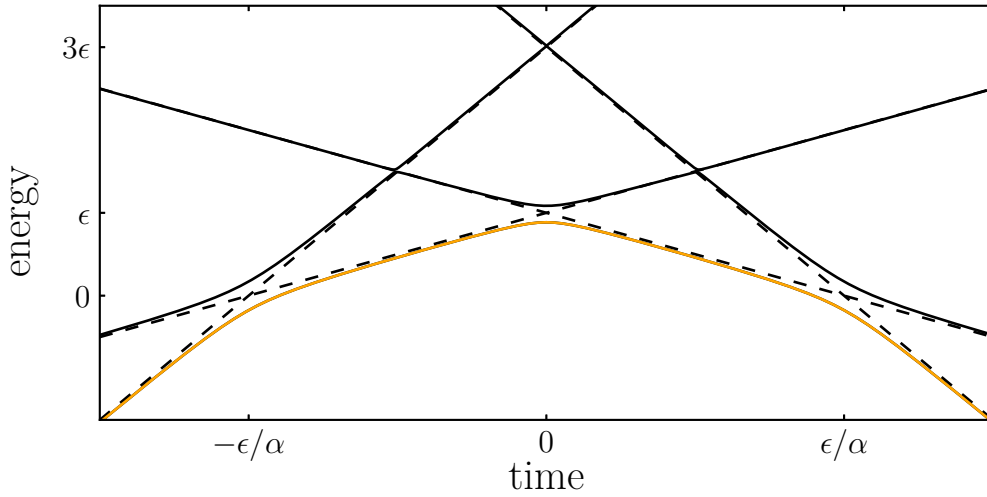


Figure 5.1: Schematic of the time-dependent spectrum of $H(t)$. Dashed and solid lines represent diabatic and adiabatic eigenstates, respectively. The temporal evolution of the ground state subject to superadiabatic control is given by the orange line. The specific configuration of parameters is $\alpha = \Delta = 1$, $\epsilon = 10$.

Our choice of generalized Hamiltonian is

$$H(t) = \begin{pmatrix} 3(\epsilon + \alpha t) & \sqrt{3}\Delta & 0 & 0 \\ \sqrt{3}\Delta & \epsilon + \alpha t & \Delta & 0 \\ 0 & \Delta & \epsilon - \alpha t & \sqrt{3}\Delta \\ 0 & 0 & \sqrt{3}\Delta & 3(\epsilon - \alpha t) \end{pmatrix}. \quad (5.1)$$

For $\epsilon \equiv 0$ it can be written in terms of spin-3/2 operators as

$$H(t) = 2\alpha t S_z + 2\Delta S_x. \quad (5.2)$$

The time-dependent spectrum is shown in Fig. 5.1. Steering the ground state by the sequential control protocol now involves the correction of non-adiabatic terms at three direct ACs. All three ACs happen at the same effective sweep rate, while the left (L) and right (R) ACs couple stronger than the central (C) one. Note that the individual direct ACs are separated by ϵ/α , while in the three-level no central ACs is present and therefore the separation is $2\epsilon/\alpha$.

As described in Sec. 3.3.1 we can now transform into the local eigenbasis at each ACs and find the unitary transformation that diagonalizes the two-by-two submatrix of $H(t)$. The elements of the resulting local CD Hamiltonians constitute the individual control pulses that are given by the Lorentzians

$$f_{L/R}(t) = \frac{1}{2} \frac{\sqrt{3}\Delta\alpha}{3\Delta^2 + (\alpha t \pm \epsilon)^2} \quad \text{and} \quad f_C(t) = \frac{1}{2} \frac{\Delta\alpha}{\Delta^2 + (\alpha t)^2}. \quad (5.3)$$

In analogy to the three-state system, we construct the ideal and realistic SC Hamiltonians by

$$H_{\text{ideal}}(t) = i \begin{pmatrix} 0 & -f_L(t) & 0 & 0 \\ f_L(t) & 0 & -f_C(t) & 0 \\ 0 & f_C(t) & 0 & -f_R(t) \\ 0 & 0 & f_R(t) & 0 \end{pmatrix} \quad (5.4)$$

and

$$H_{\text{real}}(t) = 2g(t)S_y = ig(t) \begin{pmatrix} 0 & -\sqrt{3} & 0 & 0 \\ \sqrt{3} & 0 & -1 & 0 \\ 0 & 1 & 0 & -\sqrt{3} \\ 0 & 0 & \sqrt{3} & 0 \end{pmatrix}, \quad (5.5)$$

where

$$g(t) = \frac{1}{\sqrt{3}}f_L(t) + f_C(t) + \frac{1}{\sqrt{3}}f_R(t). \quad (5.6)$$

As in the three-level case we are interested in the fidelity of the protocols in terms of the probability of non-adiabaticity. It is plotted in Fig. 5.2 for the ideal (top plot) and realistic (bottom plot) versions. Importantly, the overall situation is comparable to the three-level case: In both cases the afidelity features jumps and oscillations located at the AC times. For the realizable version these are extremely enhanced, still $\mathcal{P}(t \rightarrow \infty)$ at the end of the protocol is surprisingly small and about ten times larger than in the ideal scenario. The fact that the error of the realizable protocol is maximal at the origin can only be due to the fact that the remaining levels also cross in an indirect AC event.

We finish our studies by extracting the dependency of the afidelity on the inter-separation parameter ϵ as is shown in Fig. 5.3. We immediately note that the curves are not as smooth as for the three-level case (compare Fig. 4.5). Especially the

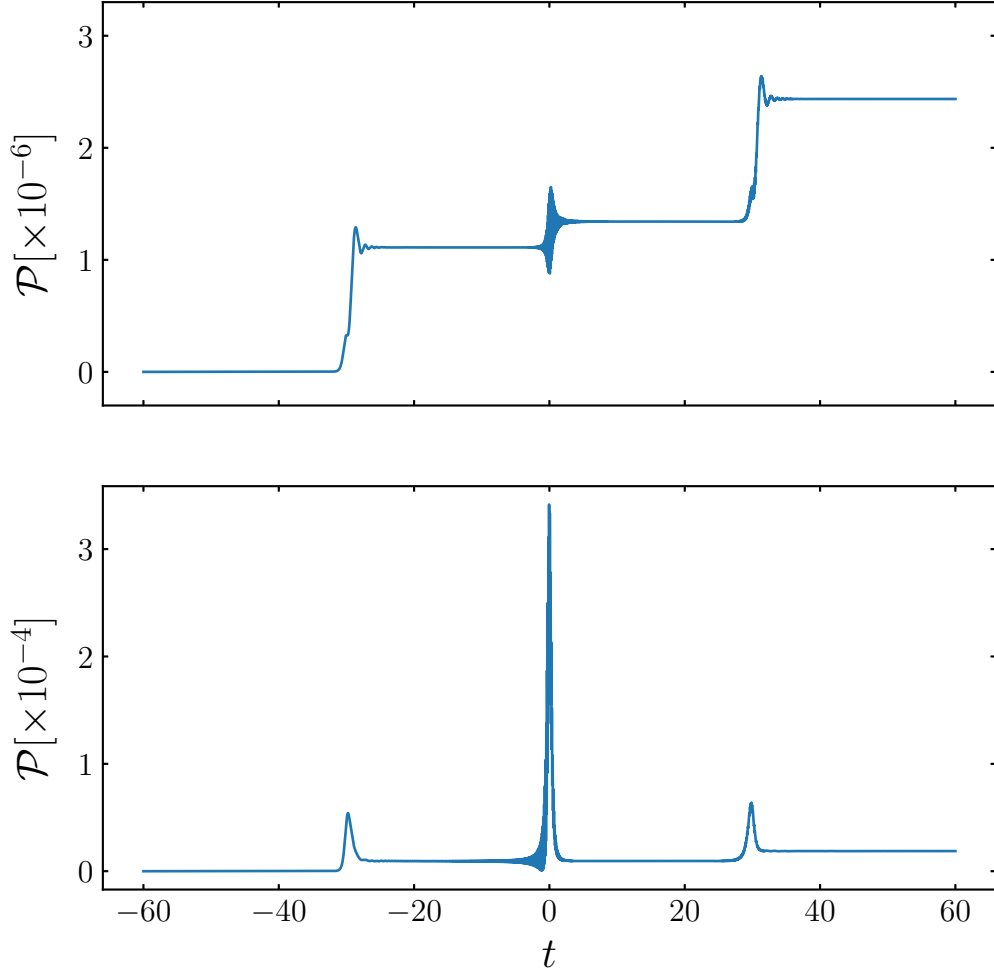


Figure 5.2: Effects of the ideal (top) and realizable (bottom) SC Hamiltonians on the system's dynamics. The error of the respective protocols as defined by the probability of non-adiabaticity (4.2) is shown. Parameters are: $\alpha = 1$, $\Delta = 0.5$, $\epsilon = 30$.

afidelity of the realizable (orange line) protocol oscillates quickly for small ϵ . However, just as in the three-level case both SC protocols scale ϵ^{-2} for large separations. Therefore, we say they achieve approximate driving of the instantaneous ground state in terms of occupation numbers. For a desired precision of $\mathcal{P} \sim 10^{-4}$, we extract the critical values of the separation to be $\epsilon \sim 5$ for the ideal and $\epsilon \sim 13$ for the realizable SC protocol.

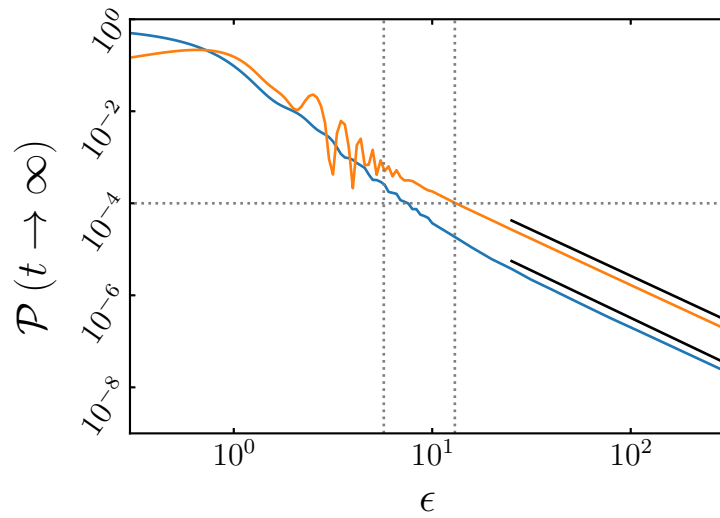


Figure 5.3: Asymptotic (large t) probability of non-adiabaticity as a function of separation parameter ϵ . Orange and blue lines correspond to ideal and realistic sequential control protocols. The power law fits for large ϵ are shifted for better visibility. The dashed lines highlight the threshold separations for $\mathcal{P} \sim 10^{-4}$. Parameters are: $\alpha = 1$, $\Delta = 0.5$.

6 Conclusion

In this thesis, we developed a type of control protocol that achieves approximate adiabatic driving of a three-level quantum system in the case where the instantaneous ground state undergoes sequential avoided crossings. We motivated our quest by discussing transitionless quantum driving theory for the two-level system; its theoretical background, experimental success and also limitations. Namely, the counterdiabatic protocol suppresses non-adiabatic transitions between eigenstates via Lorentzian pulses located at the avoided crossings. However, exact superadiabatic driving requires knowledge of the instantaneous eigenstates of a quantum system which are in general not accessible for few-level systems.

We therefore asked the question whether it is possible to decompose the global control task into individual two-level control scenarios acting at the avoided crossings where the probability of non-adiabaticity is largest. In order to study this possibility we modelled an idealized three-level system whose ground state passes two sequential Landau-Zener events. Numerical studies of the exact superadiabatic protocol for this system revealed that the control Hamiltonian indeed features peaks located at the avoided crossings. Using perturbation theory we showed that these peaks can be approximated as Lorentzian curves and that the asymptotic behaviour of the exact control functions is accordingly governed by a power law t^{-2} . On the one hand, this validates the approximation of the control pulses as Lorentzians as the asymptotic scaling behaviour is equal, but on the other hand denies a notion of perfect separability of the avoided crossing events, as no natural interaction scale can be defined.

Nonetheless, we studied the effects of such “sequential control” protocols, in the dynamic scenario. Numerical propagation indicated that the constructed protocol indeed drives the population of the instantaneous ground state close to unity. Also, we discovered that in the asymptotic time limit the probability of non-adiabaticity scales as a power law with the separation of the avoided crossings. Thus the presented protocol can achieve approximate adiabatic quantum driving in the limit of perfectly isolated single avoided crossing events. We like to mention that we already published the results for the three-level system in a shortend version ([Theisen et al., 2017](#)). Here, we further argued that the idea of sequential control may easily be adopted to arbitrary numbers of energy levels and driving of any instantaneous eigenstate. This assumption was tested and found valid for a particular four-level system which features three direct avoided crossings of the ground state.

Finally, we discussed ways to implement the protocol in physical systems. In particular we modified our protocol to comply with experimental constraints and showed that the model is most likely realizable in effective spin-1 systems or Bose-Einstein condensates in optical lattices.

A successful realization of the protocol could find application in a variety of quantum technologies. In particular adiabatic quantum computing demands efficient, that is fast and reliable, protocols that drive the adiabatic states transitionlessly. In view of those requirements, we suggest to improve our sequential control with quantum error correction techniques ([Terhal, 2015](#)). Further, we imagine possible usage in qutrit and two-qubit quantum gate implementation ([Paul and Sarma,](#)

2016). Note, that the our model of a three-level system could also be read as the sequential application of two single qubit operations in the presence of a auxiliary third state. Our results on separability then give an effective estimate on whether the single operations can be treated as individual events and how they effect each other.

In concluding we want to give future prospects. An interesting question is the generalization to even higher-level systems, particularly in view of the error scaling. Does a reasonable restriction exist on how many avoided crossings can be controlled by the proposed protocol? How does the presence of additional close states affect the dynamics? Another aspect would be the improvement of the current protocol and its recasting to alternate physically realizable forms. Is it possible to approximately drive the relative phase as well? Can we control indirect avoided crossings in order to allow for possitive probability feedback?

Eventually, I like to thank the WuTGe for their everlasting support - I love you all - and further Francesco Petiziol - Yeah Bro - as well as my supervisor Sandro Wimberger for their realistic relativation of aspirations and fruitfull discussions.

Part
Appendix

A Derivation of Landau-Zener Formula

In this appendix we first derive the equations governing the dynamics of a general two-state system and then solve them for the LZ problem and deduce the LZ formula. For the later we closely follow the work of [Majorana \(1932\)](#).

If the two-state system is time-dependent, the Hamiltonian (2.19) evaluated at different times may not commute and the time evolution operator has the general form (2.6). We therefore fall back to the Schrödinger equation (2.5) which results in a set of coupled differential equations for the diabatic expansion coefficients:

$$i\dot{c}_1 = \omega c_1 + \Delta c_2, \quad (\text{A.1a})$$

$$i\dot{c}_2 = \Delta^* c_1 - \omega c_2. \quad (\text{A.1b})$$

For simplicity, we treat the case where $\Delta \equiv |\Delta|$ is a real function of time. We then introduce a new set of coefficients by

$$d_1(t) = \exp\left\{+i \int \omega dt\right\} c_1(t) \quad \text{and} \quad d_2(t) = \exp\left\{-i \int \omega dt\right\} c_2(t). \quad (\text{A.2})$$

The modified differential equations read:

$$i\dot{d}_1 = \Delta \exp\left\{+i \int \omega dt\right\} d_2, \quad (\text{A.3a})$$

$$i\dot{d}_2 = \Delta \exp\left\{-i \int \omega dt\right\} d_1. \quad (\text{A.3b})$$

Differentiating and inserting (A.3) yields the decoupled second-order differential equations:

$$\ddot{d}_1 - \left(\frac{\dot{\Delta}}{\Delta} + i\omega\right) \dot{d}_1 + \Delta^2 d_1 = 0, \quad (\text{A.4a})$$

$$\ddot{d}_2 - \left(\frac{\dot{\Delta}}{\Delta} - i\omega\right) \dot{d}_2 + \Delta^2 d_2 = 0. \quad (\text{A.4b})$$

We now solve the special case where the interaction is time-independent $\dot{\Delta} = 0$ and the energy sweep function is linear $\omega(t) = \alpha t$ with $\alpha > 0$. For this specific problem the equations become:

$$\ddot{d}_1 - i\alpha t \dot{d}_1 + \Delta^2 d_1 = 0, \quad (\text{A.5a})$$

$$\ddot{d}_2 + i\alpha t \dot{d}_2 + \Delta^2 d_2 = 0. \quad (\text{A.5b})$$

As the coefficients are connected via the normalization constraint $|d_1|^2 + |d_2|^2 = 1$ we can focus on solving either of the above equations. By letting

$$\tilde{d} = \exp\left\{i\frac{\alpha t^2}{4}\right\}d_2 \quad (\text{A.6})$$

the second equation becomes

$$\ddot{\tilde{d}} + \left(\frac{(\alpha t)^2}{4} - i\frac{\alpha}{2} + \Delta^2\right)\tilde{d} = 0. \quad (\text{A.7})$$

Now by the change of variables

$$z = \sqrt{\alpha} \exp\left\{-\frac{\pi}{4}\right\}t, \quad \nu = i\frac{\Delta^2}{\alpha} \quad (\text{A.8})$$

Eq. (A.7) can be brought into standard form

$$\partial_z^2 \tilde{d} + \left(\nu + \frac{1}{2} - \frac{z^2}{4}\right)\tilde{d} = 0. \quad (\text{A.9})$$

This is the Weber differential equation which has two independent solutions $\tilde{d} = D_{-\nu-1}(-iz)$ and $\tilde{d} = D_\nu(z)$, where $D_\nu(z)$ is the parabolic cylinder function. Therefore, the general solution for the original coefficients from Eq. (A.1) is found by superposing both solutions and resubstituting the defined expressions

$$c_2(t) = (aD_{-\nu-1}(-i\sqrt{\alpha}e^{-\pi/4}t) + bD_\nu(\sqrt{\alpha}e^{-\pi/4}t))e^{+i\alpha t^2/4}. \quad (\text{A.10})$$

Here, a and b are determined by the initial conditions.

As we are interested in the non-adiabatic population transfer induced by the crossing, we demand that initially only one diabatic state is occupied, let us say $|2\rangle$. The probability of non-adiabatic transition is then given by $|\langle 2|\Psi(t)\rangle|^2$.

Then, the asymptotic solution for $t \rightarrow \pm\infty$ is found by regarding the asymptotic expansion of the parabolic cylinder functions as found in [Gradstheyn and Ryzhik \(2014\)](#). Accordingly,

$$\begin{aligned} \mathcal{P}_{LZ} &= |c_2(t \rightarrow \infty)|^2 \\ &= \exp\left\{-2\pi\frac{\Delta^2}{\alpha}\right\}. \end{aligned} \quad (\text{A.11})$$

This expression for the probability of non-adiabatic transition is called the *Landau-Zener formula*. This formula is also valid for complex couplings, by taking the absolute value $|\Delta|$. As shown by [Wittig \(2005\)](#) equation (A.5) can directly be solved by contour integration to yield P_{LZ} for the given initial conditions.

B Derivation of CD Hamiltonian at $t = 0$

In this appendix we derive exact expressions for the control elements of $H_{CD}(t = 0)$. Consider the three-level system (3.13) at time $t = 0$. The corresponding Hamiltonian

$$H(0) = \begin{pmatrix} \epsilon & \Delta_1 & 0 \\ \Delta_1 & 0 & \Delta_2 \\ 0 & \Delta_2 & \epsilon \end{pmatrix} \quad (\text{B.1})$$

is diagonalizable by analytic means and permits real-algebraic expressions for the eigenvalues and (instantaneous) eigenstates. The former are given by

$$\lambda_0 \equiv \epsilon, \quad \lambda_{\pm} = \frac{1}{2} \left(\epsilon \pm \sqrt{\epsilon^2 + 4(\Delta_1^2 + \Delta_2^2)} \right), \quad (\text{B.2})$$

and the eigenstates are the columns of the corresponding transformation matrix

$$U = (|\lambda_{-}\rangle \quad |\lambda_0\rangle \quad |\lambda_{+}\rangle) = \begin{pmatrix} \Delta_1/k_{+} & -\Delta_2/\Delta & \Delta_1/k_{-} \\ -\lambda_{+}/k_{+} & 0 & -\lambda_{-}/k_{-} \\ \Delta_2/k_{+} & \Delta_1/\Delta & \Delta_2/k_{-} \end{pmatrix}, \quad (\text{B.3})$$

where we defined the following quantities for simplification purposes

$$\Delta = \sqrt{\Delta_1^2 + \Delta_2^2}, \quad k = \sqrt{\epsilon^2 + 4\Delta^2} \quad \text{and} \quad k_{\pm} = \sqrt{\lambda_{\pm}^2 + \Delta^2}. \quad (\text{B.4})$$

Note that U is orthogonal (unitary) but not hermitian. Before advancing let us give some identities that will come in handy later:

$$\begin{aligned} \lambda_{\pm} + \lambda_{\mp} &= \epsilon & \lambda_{\pm}\lambda_{\mp} &= -\Delta^2 & k_{\pm}^2 + k_{\mp}^2 &= k^2 \\ \lambda_{\pm} - \lambda_{\mp} &= \pm k & k_{\pm}k_{\mp} &= \Delta k & k_{\pm}^2 - k_{\mp}^2 &= \pm \epsilon k \end{aligned} \quad (\text{B.5})$$

With the eigenvalues and eigenstates at hand we can now compute the CD Hamiltonian at $t = 0$ according to Eq. (2.29). In particular the individual control elements in the eigenbasis of $H(0)$, as indicated by the superscript λ , are given by

$$(H_{CD}^{\lambda})_{ij}(0) = i \frac{(U^{\dagger}(\partial_t H(0))U)_{ij}}{\lambda_j - \lambda_i}. \quad (\text{B.6})$$

Here $\partial_t H(0)$ describes the time derivative

$$\partial_t H(t) = \begin{pmatrix} \alpha & 0 & 0 \\ 0 & 0 & 0 \\ 0 & 0 & -\beta \end{pmatrix} \quad (\text{B.7})$$

evaluated at the origin. However, due to the linearity in our model this matrix is constant for all times. Note that by definition H_{CD}^λ is hermitian and has zeros on the diagonal. Therefore we can focus on calculating the elements of the upper triangular matrix.

For clarity we explicitly compute one coupling element:

$$\begin{aligned} (H_{CD}^\lambda)_{12} &= i \frac{1}{\Delta k_+ (\lambda_0 - \lambda_-)} \begin{pmatrix} \Delta_1 \\ -\lambda_+ \\ \Delta_2 \end{pmatrix}^T \cdot \begin{pmatrix} \alpha & 0 & 0 \\ 0 & 0 & 0 \\ 0 & 0 & -\beta \end{pmatrix} \cdot \begin{pmatrix} -\Delta_2 \\ 0 \\ \Delta_1 \end{pmatrix} \\ &= -i \frac{\Delta_1 \Delta_2 (\alpha + \beta)}{\Delta k_+ \lambda_+} \end{aligned} \quad (\text{B.8})$$

Similarly we find:

$$(H_{CD}^\lambda)_{13} = i \frac{\alpha \Delta_1^2 - \beta \Delta_2^2}{\Delta k^2}, \quad (\text{B.9})$$

$$(H_{CD}^\lambda)_{23} = i \frac{\Delta_1 \Delta_2 (\alpha + \beta)}{\Delta k_- \lambda_-}. \quad (\text{B.10})$$

Finally, we transform back into the original basis as $H_{CD} = U H_{CD}^\lambda U^\dagger$. Although the diagonals of H_{CD}^λ are zero this is not necessarily true for H_{CD} . However in our case the transformation matrix U is real-valued and to ensure hermiticity of the Hamiltonian in all bases the diagonals must vanish. After some basic algebra and by using the identities (B.5), the remaining independent elements take the values:

$$(H_{CD})_{12} = i \frac{\Delta_1 (\alpha \Delta_1^2 - \beta \Delta_2^2)}{\Delta^2 k^2} + i \frac{\Delta_1 \Delta_2^2 (\alpha + \beta)}{\Delta^4}, \quad (\text{B.11})$$

$$(H_{CD})_{13} = i \frac{\Delta_1 \Delta_2 \epsilon (\alpha + \beta)}{\Delta^4}, \quad (\text{B.12})$$

$$(H_{CD})_{23} = -i \frac{\Delta_2 (\alpha \Delta_1^2 - \beta \Delta_2^2)}{\Delta^2 k^2} + i \frac{\Delta_1^2 \Delta_2 (\alpha + \beta)}{\Delta^4}. \quad (\text{B.13})$$

There are two interesting things to be noted. First, we notice that for the $\alpha \Delta_1 = \beta \Delta_2$ the first term in the expressions of $(H_{CD})_{12}$ and $(H_{CD})_{23}$ vanishes. This is particularly the case for the spin-1 system, where $\alpha = \beta$ and $\Delta_1 = \Delta_2$. Second and in contrary to the spin-1 system, we see that the $(H_{CD})_{13}$ element is not zero and depends linearly on the offset ϵ .

C Time-Independent Perturbation Theory

In this appendix we sketch how to use time independent perturbation theory (TIPT) to calculate the CD control Hamiltonian. In particular, we derive the control elements in the case of weak coupling and in the asymptotic (large t) limit.

Let H be a Hamiltonian whose eigenvalue problem is not analytically solvable. In order to approximate the exact solution, i.e., the eigenenergies E_n and eigenstates $|E_n\rangle$, we decompose the Hamiltonian into two parts

$$H = H_0 + H_1, \quad (\text{C.1})$$

such that H_0 is solvable with the eigenvalues and eigenstates given by $E^{(0)}$ and $|E^{(0)}\rangle$, respectively. We can now apply perturbation theory to derive approximate solutions by treating H_1 as a small perturbation. Usually, this is done by writing

$$H_1 = \lambda V \quad (\text{C.2})$$

and assuming the perturbation parameter $\lambda \in \mathbb{R}$ to be small. We next expand the exact solution in orders of λ :

$$E_n = \sum_{k=0}^{\infty} \lambda^k E_n^{(k)} \quad (\text{C.3})$$

$$|E_n\rangle = \sum_{k=0}^{\infty} \lambda^k |E_n^{(k)}\rangle. \quad (\text{C.4})$$

Here, $E_n^{(k)}$ and $|E_n^{(k)}\rangle$ are the k -order correction terms to E_n and $|E_n\rangle$. As described in [Sakurai and Napolitano \(2011\)](#), they can then be calculated recursively by

$$E_n^{(j)} = \langle E_n^{(0)} | V | E_n^{(j-1)} \rangle - \sum_{k=1}^{j-1} E_n^{(k)} \langle E_n^{(0)} | E_n^{(j-k)} \rangle \quad (\text{C.5})$$

and

$$|E_n^{(j)}\rangle = \sum_m \langle E_m^{(0)} | E_n^{(j)} \rangle |E_m^{(0)}\rangle. \quad (\text{C.6})$$

The matrix elements in the later expression are computed for $m \neq n$ by

$$\langle E_m^{(0)} | E_n^{(j)} \rangle = -\frac{\langle E_m^{(0)} | V | E_n^{(j-1)} \rangle}{E_m^{(0)} - E_n^{(0)}} + \sum_{k=1}^{j-1} \frac{E_n^{(k)} \langle E_m^{(0)} | E_n^{(j-k)} \rangle}{E_m^{(0)} - E_n^{(0)}} \quad (\text{C.7})$$

and for $m = n$ by

$$\langle E_n^{(0)} | E_n^{(j)} \rangle = -\frac{1}{2} \sum_{k=1}^{j-1} \langle E_n^{(j-k)} | E_n^{(k)} \rangle. \quad (\text{C.8})$$

Note that the later element ensures normalization of the approximate states. The perturbative approach we use here is applicable in the case where the energy spectrum of H_0 is non-degenerate and the perturbation V time-independent.

The CD control Hamiltonian is independent of the system's dynamics since it only depends on the instantaneous eigenstates as is evident from (2.29). With the instantaneous eigenstates from TIPT, we can therefore calculate the approximate control fields according to (2.30).

Weak Coupling Consider the instantaneous eigenvalue problem for the Hamiltonian (3.13) with a general energy sweep function $\omega(t)$. We can solve it approximately in the weak coupling limit (Δ small):

$$\left[\underbrace{\begin{pmatrix} \epsilon + \omega(t) & 0 & 0 \\ 0 & 0 & 0 \\ 0 & 0 & \epsilon - \omega(t) \end{pmatrix}}_{H_0(t)} + \Delta \underbrace{\begin{pmatrix} 0 & 1 & 0 \\ 1 & 0 & 1 \\ 0 & 1 & 0 \end{pmatrix}}_V \right] |E_n(t)\rangle = E_n(t) |E_n(t)\rangle. \quad (\text{C.9})$$

The perturbation V is time independent and therefore TIPT can be applied to solve the equation. The instantaneous eigenstates to the unperturbed system are exactly the diabatic states

$$|E_1^{(0)}\rangle = |1\rangle, \quad |E_2^{(0)}\rangle = |2\rangle, \quad |E_3^{(0)}\rangle = |3\rangle, \quad (\text{C.10})$$

where the labeling is chosen such that

$$E_1^{(0)} = \epsilon + \omega(t), \quad E_2^{(0)} = 0, \quad E_3^{(0)} = \epsilon - \omega(t). \quad (\text{C.11})$$

Further, note that the spectrum of $H_0(t)$ is degenerate at times for which $\omega(t) = \pm\epsilon$. Thus, the perturbative approach breaks down when two diabatic states cross in the spectrum. However, with the knowledge we still can approximate the solution.

Computing the eigenvectors up to second order in Δ gives

$$|E_1(t)\rangle \simeq \left(1 - \frac{\Delta^2}{2(\epsilon + \omega)^2}\right) |1\rangle + \frac{\Delta}{\epsilon + \omega} |2\rangle + \frac{\Delta^2}{2\omega(\epsilon + \omega)} |3\rangle \quad (\text{C.12})$$

$$|E_2(t)\rangle \simeq -\frac{\Delta}{\epsilon + \omega} |1\rangle + \left(1 - \frac{(\epsilon^2 + \omega^2)}{(\epsilon^2 - \omega^2)^2} \Delta^2\right) |2\rangle - \frac{\Delta}{\epsilon - \omega} |3\rangle \quad (\text{C.13})$$

$$|E_3(t)\rangle \simeq -\frac{\Delta^2}{2\omega(\epsilon - \omega)} |1\rangle + \frac{\Delta}{\epsilon - \omega} |2\rangle + \left(1 - \frac{\Delta^2}{2(\epsilon - \omega)^2}\right) |3\rangle. \quad (\text{C.14})$$

From this we calculate the CD control Hamiltonian which yields:

$$(H_{CD})_{12} = i\frac{\dot{\omega}}{(\epsilon + \omega)^2}\Delta + \mathcal{O}(\Delta^3), \quad (\text{C.15a})$$

$$(H_{CD})_{23} = i\frac{\dot{\omega}}{(\epsilon - \omega)^2}\Delta + \mathcal{O}(\Delta^3), \quad (\text{C.15b})$$

$$(H_{CD})_{13} = i\frac{\dot{\omega}\epsilon(\epsilon^2 - 5\omega^2)}{2\omega^2(\epsilon^2 - \omega^2)^2}\Delta^2 + \mathcal{O}(\Delta^3). \quad (\text{C.15c})$$

As can be seen, the expressions include singularities at the crossings $\omega = \pm\epsilon$ due to the degeneracy of the unperturbed system H_0 .

Asymptotic Limit Consider the instantaneous eigenvalue problem for the general asymmetric Hamiltonian (3.13)

$$H(t) |E_n(t)\rangle = E_n(t) |E_n(t)\rangle. \quad (\text{C.16})$$

Dividing by t and explicitly separating the Hamiltonian into time-independent H_0 and time-dependent $H_1 = V/t$ parts gives

$$\left[\underbrace{\begin{pmatrix} \alpha & 0 & 0 \\ 0 & 0 & 0 \\ 0 & 0 & -\beta \end{pmatrix}}_{H_0} + \frac{1}{t} \underbrace{\begin{pmatrix} \epsilon & \Delta_L & 0 \\ \Delta_L & 0 & \Delta_R \\ 0 & \Delta_R & \epsilon \end{pmatrix}}_V \right] |E_n(t)\rangle = \frac{E_n(t)}{t} |E_n(t)\rangle. \quad (\text{C.17})$$

Here, we assume $\alpha, \beta > 0$ to avoid degeneracy of H_0 . By rescaling the energy by $\mathcal{E}_n(t) = E_n(t)/t$ and defining $\lambda = 1/t$ the equation is brought into the canonical form

$$(H_0 + \lambda V) |E_n(t)\rangle = \mathcal{E}_n(t) |E_n(t)\rangle. \quad (\text{C.18})$$

Note that the instantaneous eigenstates are the same as for the original problem (C.16). Neither H_0 nor V depend on time and therefore the solution to this equation can be attained from time-independent perturbation theory for small values of the perturbation parameter λ . The off-diagonal matrix elements of the control Hamiltonian, We can now apply the general procedure described above to compute the eigenvectors in the large t limit.

The zeroth-order solution is attained by solving the unperturbed eigenequation

$$H_0 |E_n^{(0)}\rangle = \mathcal{E}_n^{(0)} |E_n^{(0)}\rangle. \quad (\text{C.19})$$

In this limit of $t \rightarrow \infty$, the eigenstates are exactly given by the time-independent diabatic basis states

$$\left|E_1^{(0)}\right\rangle = |3\rangle, \quad \left|E_2^{(0)}\right\rangle = |2\rangle, \quad \left|E_3^{(0)}\right\rangle = |1\rangle. \quad (\text{C.20})$$

Here, the eigenstates are labeled by increasing eigenvalues

$$\mathcal{E}_1^{(0)} = -\beta, \quad \mathcal{E}_2^{(0)} = 0, \quad \mathcal{E}_3^{(0)} = \alpha. \quad (\text{C.21})$$

Then, the eigenstates to third order read

$$\begin{aligned} |E_1(t)\rangle &\simeq \left(1 - \frac{\Delta_1^2}{2\alpha^2 t^2} + \frac{\Delta_1^2 \epsilon}{\alpha^3 t^3}\right) |3\rangle \\ &+ \left(\frac{\Delta_1}{\alpha t} - \frac{\Delta_1 \epsilon}{\alpha^2 t^2} - \frac{\Delta_1(3\Delta_1^2 - 2\epsilon^2)}{2\alpha^3 t^3} + \frac{\Delta_1 \Delta_2^2}{\alpha^2(\alpha + \beta)t^3}\right) |2\rangle \\ &+ \left(\frac{\Delta_1 \Delta_2}{\alpha(\alpha + \beta)t^2} - \frac{\Delta_1 \Delta_2 \epsilon}{\alpha^2(\alpha + \beta)t^3}\right) |1\rangle \end{aligned} \quad (\text{C.22})$$

$$\begin{aligned} |E_2(t)\rangle &\simeq \left(-\frac{\Delta_1}{\alpha t} + \frac{\Delta_1 \epsilon}{\alpha^2 t^2} + \frac{\Delta_1 \Delta_2^2(\alpha - 2\beta)}{2\alpha^2 \beta^2 t^3} + \frac{\Delta_1(3\Delta_1^2 - 2\epsilon^2)}{2\alpha^3 t^3}\right) |3\rangle \\ &+ \left(1 - \frac{\Delta_1^2}{2\alpha^2 t^2} - \frac{\Delta_2^2}{2\beta^2 t^2} + \frac{\epsilon(\Delta_1^2 \beta^3 - \Delta_2^2 \alpha^3)}{\alpha^3 \beta^3 t^3}\right) |2\rangle \\ &+ \left(\frac{\Delta_2}{\beta t} + \frac{\Delta_2 \epsilon}{\beta^2 t^2} - \frac{\Delta_2 \Delta_1^2(\beta - 2\alpha)}{2\alpha^2 \beta^2 t^3} - \frac{\Delta_2(3\Delta_2^2 - 2\epsilon^2)}{2\beta^3 t^3}\right) |1\rangle \end{aligned} \quad (\text{C.23})$$

$$\begin{aligned} |E_3(t)\rangle &\simeq \left(\frac{\Delta_1 \Delta_2}{\beta(\alpha + \beta)t^2} + \frac{\Delta_1 \Delta_2 \epsilon}{\beta^2(\alpha + \beta)t^3}\right) |3\rangle \\ &+ \left(-\frac{\Delta_2}{\beta t} - \frac{\Delta_2 \epsilon}{\beta^2 t^2} + \frac{\Delta_2(3\Delta_2^2 - 2\epsilon^2)}{2\beta^3 t^3} - \frac{\Delta_1^2 \Delta_2}{\beta^2(\alpha + \beta)t^3}\right) |2\rangle \\ &+ \left(1 - \frac{\Delta_2^2}{2\beta^2 t^2} - \frac{\Delta_2^2 \epsilon}{\beta^3 t^3}\right) |1\rangle \end{aligned} \quad (\text{C.24})$$

Note the high symmetry of the problem, e.g., $\langle 3|E_1(t)\rangle$ is equal to $\langle 1|E_3(t)\rangle$ by letting $\alpha \rightarrow -\beta$ and $\Delta_1 \rightarrow \Delta_2$.

The expansion is valid for $1/t$ small and thereby gives the approximate eigenstates of $H(t)$ for $t \rightarrow \infty$. From these we can calculate the CD control Hamiltonian for large times using (2.30). Note that the calculation of H_{CD} involves the time derivative of the eigenstates and therefore unavoidably raises the order of the perturbative

approach. The independent non-zero elements are

$$(H_{CD})_{12} = \frac{i\Delta_1}{\alpha t^2} - \frac{2i\Delta_1\epsilon}{\alpha^2 t^3} - \frac{i\Delta_1(4\Delta_1^2 - 3\epsilon^2)}{\alpha^3 t^4} + \frac{i\Delta_1\Delta_2^2(\alpha + 3\beta)}{\alpha^2\beta(\alpha + \beta)t^4} + \mathcal{O}(t^{-5}) \quad (\text{C.25a})$$

$$(H_{CD})_{23} = \frac{i\Delta_2}{\beta t^2} + \frac{2i\Delta_2\epsilon}{\beta^2 t^3} - \frac{i\Delta_2(4\Delta_2^2 - 3\epsilon^2)}{\beta^3 t^4} + \frac{i\Delta_1^2\Delta_2(\beta + 3\alpha)}{\alpha\beta^2(\alpha + \beta)t^4} + \mathcal{O}(t^{-5}) \quad (\text{C.25b})$$

$$(H_{CD})_{13} = \frac{i\Delta_1\Delta_2(\alpha - \beta)}{\alpha\beta(\alpha + \beta)t^3} - \frac{i\Delta_1\Delta_2\epsilon(2\alpha^2 + 2\beta^2 + \alpha\beta)}{\alpha^2\beta^2(\alpha + \beta)t^4} + \mathcal{O}(t^{-5}) \quad (\text{C.25c})$$

D Bibliography

- Alexandre Baksic, Hugo Ribeiro, and Aashish A. Clerk. Speeding up adiabatic quantum state transfer by using dressed states. *Phys. Rev. Lett.*, 116:230503, Jun 2016. doi: [10.1103/PhysRevLett.116.230503](https://doi.org/10.1103/PhysRevLett.116.230503).
- Mark G. Bason, Matthieu Viteau, Nicola Malossi, Paul Huillery, Ennio Arimondo, Donatella Ciampini, Rosario Fazio, Vittorio Giovannetti, Riccardo Mannella, and Oliver Morsch. High-fidelity quantum driving. *Nat Phys*, 8(2):147–152, feb 2012. ISSN 1745-2473. doi: [10.1038/nphys2170](https://doi.org/10.1038/nphys2170).
- Carl M. Bender. Making sense of non-Hermitian Hamiltonians. *Reports on Progress in Physics*, 70(6):947, 2007. URL <http://stacks.iop.org/0034-4885/70/i=6/a=R03>.
- M. V. Berry. Transitionless quantum driving. *Journal of Physics A: Mathematical and Theoretical*, 42(36):365303, 2009. URL <http://stacks.iop.org/1751-8121/42/i=36/a=365303>.
- S. Carretta, E. Liviotti, N. Magnani, P. Santini, and G. Amoretti. S mixing and quantum tunneling of the magnetization in molecular nanomagnets. *Phys. Rev. Lett.*, 92:207205, May 2004. doi: [10.1103/PhysRevLett.92.207205](https://doi.org/10.1103/PhysRevLett.92.207205).
- Carlton M. Caves, Christopher A. Fuchs, and Rüdiger Schack. Quantum probabilities as Bayesian probabilities. *Phys. Rev. A*, 65:022305, Jan 2002. doi: [10.1103/PhysRevA.65.022305](https://doi.org/10.1103/PhysRevA.65.022305).
- L. Childress, M. V. Gurudev Dutt, J. M. Taylor, A. S. Zibrov, F. Jelezko, J. Wrachtrup, P. R. Hemmer, and M. D. Lukin. Coherent dynamics of coupled electron and nuclear spin qubits in diamond. *Science*, 314(5797):281–285, 2006. ISSN 0036-8075. doi: [10.1126/science.1131871](https://doi.org/10.1126/science.1131871).
- Sebastian Deffner, Christopher Jarzynski, and Adolfo del Campo. Classical and quantum shortcuts to adiabaticity for scale-invariant driving. *Phys. Rev. X*, 4:021013, Apr 2014. doi: [10.1103/PhysRevX.4.021013](https://doi.org/10.1103/PhysRevX.4.021013).
- Adolfo del Campo. Shortcuts to adiabaticity by counterdiabatic driving. *Phys. Rev. Lett.*, 111:100502, Sep 2013. doi: [10.1103/PhysRevLett.111.100502](https://doi.org/10.1103/PhysRevLett.111.100502).
- Mustafa Demirplak and Stuart A. Rice. Adiabatic population transfer with control fields. *The Journal of Physical Chemistry A*, 107(46):9937–9945, 2003. doi: [10.1021/jp030708a](https://doi.org/10.1021/jp030708a).

- Marcus W. Doherty, Neil B. Manson, Paul Delaney, Fedor Jelezko, Jörg Wrachtrup, and Lloyd C.L. Hollenberg. The nitrogen-vacancy colour centre in diamond. *Phys. Rep.*, 528(1):1–45, 2013. ISSN 0370-1573. doi: [10.1016/j.physrep.2013.02.001](https://doi.org/10.1016/j.physrep.2013.02.001).
- D. Dong and I. R. Petersen. Quantum control theory and applications: a survey. *IET Control Theory Applications*, 4(12):2651–2671, December 2010. ISSN 1751-8644. doi: [10.1049/iet-cta.2009.0508](https://doi.org/10.1049/iet-cta.2009.0508).
- M. V. Gurudev Dutt, L. Childress, L. Jiang, E. Togan, J. Maze, F. Jelezko, A. S. Zibrov, P. R. Hemmer, and M. D. Lukin. Quantum register based on individual electronic and nuclear spin qubits in diamond. *Science*, 316(5829):1312–1316, 2007. ISSN 0036-8075. doi: [10.1126/science.1139831](https://doi.org/10.1126/science.1139831).
- D. Gatteschi, R. Sessoli, and J. Villain. *Molecular Nanomagnets*. Oxford University Press, 2006. ISBN 9780198567530. doi: [10.1093/acprof:oso/9780198567530.001.0001](https://doi.org/10.1093/acprof:oso/9780198567530.001.0001).
- Steffen J. Glaser, Ugo Boscain, Tommaso Calarco, Christiane P. Koch, Walter Köckenberger, Ronnie Kosloff, Ilya Kuprov, Burkhard Luy, Sophie Schirmer, Thomas Schulte-Herbrüggen, Dominique Sugny, and Frank K. Wilhelm. Training Schrödinger’s cat: quantum optimal control. *The European Physical Journal D*, 69(12):279, Dec 2015. ISSN 1434-6079. doi: [10.1140/epjd/e2015-60464-1](https://doi.org/10.1140/epjd/e2015-60464-1).
- John Goold, Marcus Huber, Arnau Riera, Lídia del Rio, and Paul Skrzypczyk. The role of quantum information in thermodynamics – a topical review. *Journal of Physics A: Mathematical and Theoretical*, 49(14):143001, 2016. URL <http://stacks.iop.org/1751-8121/49/i=14/a=143001>.
- I. S. Gradshteyn and I. M. Ryzhik. *Table of Integrals, Series and Products*. Daniel Zwillinger and Victor Moll, 2014.
- Hermann Haken. *Licht und Materie I: Elemente der Quantenoptik*. Bibliographisches Institut (BI) AG, Zürich, 1979. ISBN 3-411-01539-X.
- S. Danilin K. S. Kumar, A. Vepsäläinen and G. S. Paraoanu. Stimulated raman adiabatic passage in a three-level superconducting circuit. *Nat. Commun.*, 7(10628), 2016. doi: [10.1038/ncomms10628](https://doi.org/10.1038/ncomms10628).
- L. D. Landau. a theory of energy transfer II. *Phys. Z. Sowjetunion*, (2):46–51, 1932. Zur Theorie der Energieübertragung II [deutsch].
- Ettore Majorana. Atomi orientati in campo magnetico variabile. *Nuovo Cimento*, 9(2):43–50, 1932. ISSN 1827-6121. doi: [10.1007/BF02960953](https://doi.org/10.1007/BF02960953).
- N. Malossi, M. G. Bason, M. Viteau, E. Arimondo, R. Mannella, O. Morsch, and D. Ciampini. Quantum driving protocols for a two-level system: From generalized Landau-Zener sweeps to transitionless control. *Phys. Rev. A*, 87:012116, Jan 2013. doi: [10.1103/PhysRevA.87.012116](https://doi.org/10.1103/PhysRevA.87.012116).

- Koushik Paul and Amarendra K. Sarma. Creation of entangled states via transitionless quantum driving. In *13th International Conference on Fiber Optics and Photonics*, page W3A.30. Optical Society of America, 2016. doi: [10.1364/PHOTONICS.2016.W3A.30](https://doi.org/10.1364/PHOTONICS.2016.W3A.30).
- L. Pitaevskii and S. Stringari. *Bose-Einstein Condensation*. Oxford University Press, 2003. ISBN 9780198507192.
- J. J. Sakurai and Jim Napolitano. *Modern Quantum Mechanics*. Addison-Wesley, San Francisco, CA, 2 edition, 2011. ISBN 978-0-321-50336-7.
- S.N. Shevchenko, S. Ashhab, and Franco Nori. Landau-Zener-Stückelberg interferometry. *Phys. Rep.*, 492(1):1–30, 2010. ISSN 0370-1573. doi: [10.1016/j.physrep.2010.03.002](https://doi.org/10.1016/j.physrep.2010.03.002).
- J. C. Solem and L. C. Biedenharn. Understanding geometrical phases in quantum mechanics: An elementary example. *Foundations of Physics*, 23(2):185–195, 1993. ISSN 1572-9516. doi: [10.1007/BF01883623](https://doi.org/10.1007/BF01883623).
- E. C. G. Stückelberg. *Helv. Phys. Acta*, 5(369), 1932.
- G. Tayebirad, A. Zenesini, D. Ciampini, R. Mannella, O. Morsch, E. Arimondo, N. Lörch, and S. Wimberger. Time-resolved measurement of landau-zener tunneling in different bases. *Phys. Rev. A*, 82:013633, Jul 2010. doi: [10.1103/PhysRevA.82.013633](https://doi.org/10.1103/PhysRevA.82.013633).
- Barbara M. Terhal. Quantum error correction for quantum memories. *Rev. Mod. Phys.*, 87:307–346, Apr 2015. doi: [10.1103/RevModPhys.87.307](https://doi.org/10.1103/RevModPhys.87.307).
- M. Theisen, F. Petiziol, S. Carretta, P. Santini, and S. Wimberger. Superadiabatic driving of a three-level quantum system. *Phys. Rev. B*, 2017. accepted, to be published.
- Erik Torrontegui, Sara Ibáñez, Sofia Martínez-Garaot, Michele Modugno, Adolfo del Campo, David Guéry-Odelin, Andreas Ruschhaupt, Xi Chen, and Juan Gonzalo Muga. Shortcuts to adiabaticity. *Adv. At., Mol. Opt. Phys.*, 62:117 – 169, 2013. ISSN 1049-250X. doi: [10.1016/B978-0-12-408090-4.00002-5](https://doi.org/10.1016/B978-0-12-408090-4.00002-5).
- M V Volkov and V N Ostrovsky. Exact results for survival probability in the multi-state Landau-Zener model. *Journal of Physics B: Atomic, Molecular and Optical Physics*, 37(20):4069, 2004. URL <http://stacks.iop.org/0953-4075/37/i=20/a=003>.
- C. Wittig. The Landau-Zener formula. *The Journal of Physical Chemistry B*, 109(17):8428–8430, 2005. doi: [10.1021/jp040627u](https://doi.org/10.1021/jp040627u).

C. Zener. Non-adiabatic crossing of energy levels. *Proceedings of the Royal Society of London A: Mathematical, Physical and Engineering Sciences*, 137(833):696–702, 1932. ISSN 0950-1207. doi: 10.1098/rspa.1932.0165.

Alessandro Zenesini, Carlo Sias, Hans Lignier, Yeshpal Singh, Donatella Ciampini, Oliver Morsch, Riccardo Mannella, Ennio Arimondo, Andrea Tomadin, and Sandro Wimberger. Resonant tunneling of Bose-Einstein condensates in optical lattices. *New J. Phys.*, 10(5):053038, 2008. URL <http://stacks.iop.org/1367-2630/10/i=5/a=053038>.

B. B. Zhou, A. Baksic, H. Ribeiro, C. G. Yale, F. J. Heremans, P.C. Jerger, A. Auer, G. Burkard, A. A. Clerk, and D. D. Awschalom. Accelerated quantum control using superadiabatic dynamics in a solid-state lambda system. *Nature Phys.*, 13(330–334), 2017. doi: 10.1038/nphys3967.

Erklärung:

Ich versichere, dass ich diese Arbeit selbstständig verfasst habe und keine anderen als die angegebenen Quellen und Hilfsmittel benutzt habe.

Heidelberg, den (Datum)